Space-Time Coding for CDMA-based Wireless Communication Systems

By

Alper TABAN

A Dissertation Submitted to the Graduate School in Partial Fulfillment of the Requirements for the Degree of

MASTER OF SCIENCE

Department: Electrical and Electronics Engineering

Major: Electronics and Communication

İzmir Institute of Technology

İzmir, Turkey

August, 2002

We approve the thesis of **Alper TABAN**

Date of Signature

..... **06.08.2002**

Assist. Prof. Dr. Mustafa Aziz ALTINKAYA

Supervisor

Department of Electrical and Electronics Engineering

..... **06.08.2002**

Assist. Prof. Dr. Reyat YILMAZ

Department of Electrical and Electronics Engineering

Dokuz Eylül University

..... **06.08.2002**

Assist. Prof. Dr. Mehmet Salih DİNLEYİCİ

Department of Electrical and Electronics Engineering

..... **06.08.2002**

Prof. Dr. Ferit Acar SAVACI

Head of Department

ACKNOWLEDGEMENT

I would like to thank my supervisor Assistant Professor Dr. Mustafa Aziz Altınkaya for his support and guidance throughout my research.

I would also like to thank Assistant Professors Mehmet Salih Dinleyici and Reyat Yılmaz for serving on my thesis committee. Their advice and comments are greatly appreciated.

Finally, I would like to thank my colleagues Özgür Oruç, Berna Özbek, Funda Kurtdemir and Erdal Özbek for supplying me various helps.

ABSTRACT

Multiple transmit antennas giving rise to diversity (transmit diversity) have been shown to increase downlink (base station to the mobile) capacity in cellular systems. The third generation partnership project (3GPP) for WCDMA has chosen space time transmit diversity (STTD) as the open loop transmit diversity technique for two transmit antennas. On the other hand, the CDMA 2000 has chosen space time spreading (STS) and orthogonal transmit diversity (OTD) as the open loop transmit diversity. In addition to all the standardization aspects, proposed contributions such as space time coding assisted double spread rake receiver (STC-DS-RR) are exist.

In this thesis, open loop transmit diversity techniques of 3GPP, CDMA 2000 and existing contributions are investigated. Their performances are compared as a means of bit-error-rate (BER) versus signal-to-noise ratio (SNR).

ÖZ

Hücresel sistemlerde iletim çeşitliliğinin baz istasyonundan gezgin istasyona doğru olan iletişim kapasitesini arttırdığı gösterilmiştir. Genişband kod bölüşümlü çoklu erişim için geliştirilen üçüncü nesil ortaklık tasarısı uzay zaman iletim çeşitliliğini seçmiştir. Bunun yanında açık çevrim iletim çeşitlemesinde olduğu gibi, kod bölüşümlü çoklu erişim 2000 projesi için uzay zamanda yayılma ve dikgen verici çeşitlemesi seçilmiştir. Öngörülen bütün standartlara ek olarak, çift yaymalı tırmık almacı kullanılarak uzay zaman kodlama sistemi gibi önerilen katkılar da vardır.

Bu tezde, üçüncü nesil ortaklık tasarısı, kod bölüşümlü çoklu erişim 2000 projesi ve diğer çalışmaların açık çevrim verici çeşitleme teknikleri incelenmiştir. Bu sistemlerin performansları bit hata oranına karşı işaret gürültü oranı şeklinde karşılaştırılmıştır.

TABLE OF CONTENTS

LIST OF FIGURES

LIST OF TABLES

C H A P T E R 1

INTRODUCTION

There is a growing trend in the communications market towards wireless systems. The removal of the physical link between a user and the remainder of the communication system permits greater user mobility and requires less physical infrastructure, which thereby reduces the overall system cost. Next-generation cellular phone systems will be of a digital form for an improved quality of service. Since there is a finite amount of the radio spectrum available for cellular purposes, it is desirable to accommodate as many users as possible within that bandwidth, while not compromising the level of performance. CDMA (Code Division Multiple Access) is one technique by which a given portion of the radio spectrum can be shared among multiple users. TDMA (Time Division Multiple Access) and FDMA (Frequency Division Multiple Access) are two other multiple access techniques, which provide separate time slots or frequency bands, respectively, for different users. The major disadvantage of both TDMA and FDMA is that they are both limited to a specific maximum number of users by the number of available time slots or frequency channels. In addition, adjacent cells cannot share the same channel allocations due to mutual interference. Conversely, in CDMA, all of the users share the same bandwidth with each mobile's signal being spread by a unique individual PN (pseudo-noise) chip sequence. By correlating the received signal at the base station with each user's known sequence, the original data can be recovered. Unlike the other two methods, CDMA is limited only by interference (which arises mainly from other users). Thus, instead of having a sharp cut off point in cell capacity, it is possible to continue adding users to the system by gradually reducing everyone's level of performance. [1] provides a good introduction to the concept of cellular CDMA and illustrates how this multiple-access scheme is more suitable for the cellular environment than are TDMA and FDMA, in terms of providing greater system capacity.

The growth rate of the mobile industry pushes the new innovations so today we reach Wideband Code Division Multiple Access (WCDMA) standards within the Third Generation Partnership Project (3GPP). These wideband systems will provide access

speeds ranging from a few hundred kbits/s for full mobility wide area access, up to 2Mbits/s in local areas with low mobility [2]. Achieving such high data rates in radio channels which are inherently limited by severe distortions such as multipath propagation and signal fading, is a challenging task. Antenna arrays have been proposed as a means to improve performance in both links of CDMA systems. On the uplink, the capacity can be improved by employing multiple-antenna diversity techniques, multiuser detection (MUD) or interference cancellation. On the downlink, the size and power consumption limitations of the mobile terminal effectively put restrictions on the complexity of the receivers that can be implemented, and, thus, on the capacity. However, since future multimedia services will place higher demands on the downlink than on the uplink, it is important to find techniques that can boost the capacity of the downlink channel. Base station transmit antenna diversity has been identified as an efficient way of improving the capacity without expanding the bandwidth, especially in low-mobility environments where there is in-sufficient time or frequency diversity [3], [4]. Indeed, transmit diversity has already been adopted by the 3GPP standards [5]. The standards specify the transmission format and certain performance requirements, but leaves room for manufacturers and operators to implement individual data receiver solutions.

The aim of this thesis is to investigate and compare existing transmit diversity schemes which utilize some form of space-time coding for CDMA-based systems in flat fading and multipath channels. This thesis is organized as follows. Chapter 2 introduces the fundamentals of wireless channel properties, large-scale path loss, small-scale path loss, Multiple Input Multiple Output (MIMO) channels. Chapter 3 provides a detailed survey of the CDMA subsystems. Advantages of CDMA over TDMA and FDMA are presented. Examples of spread spectrum systems are classified and types of spreading sequences are described. Chapter 4 presents an introduction to space-time block codes. Chapter 5 gives detailed aspects of transmit diversity techniques in CDMA system. The differences of these systems are analyzed in terms of bit error probability. In chapter 6, simulation concepts and their results are presented. The simulation results obtained with various techniques using a common channel model are compared. Concluding remarks are given in chapter 7.

CHAPTER 2

WIRELESS CHANNEL

2.1 Introduction

Communication in a wireless environment has many kind of problems, which the main concern is to compensate for degradation due to additive white Gaussian noise. In the wireless environment we must account for, shadowing caused by obstructions between the transmitter and receiver, and fading due to the constructive and destructive interference of multiple reflected paths. Figure 2.1 depicts the effects of the wireless channel on propagating signals in its environment. There is a large loss in received power that is proportional to the square of the distance between the transmitter and receiver. This loss is normally known as free space loss.

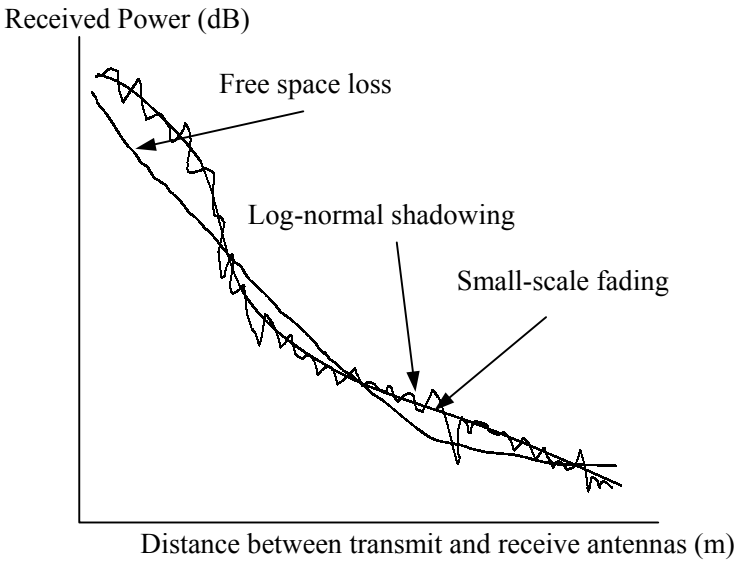

Figure 2.1 Effects on received signal power in a wireless or fading channel

There is also some gradual variation about the free space loss due to variable numbers of objects in the signal path at different locations and times. This large-scale variation will be

modeled as log-normal shadowing. The final component of signal degradation is the rapid fluctuation in signal power primarily due to the relative motion between the receiver and transmitter. This is described as small-scale fading and can be modeled in several ways. In this section our main interest is to show how small-scale fading effects communication performance. Hence we will discuss more detailed on this subject in this chapter in order to understand and model the wireless channel.

2.2 Small-Scale Path Loss

While large-scale path loss describes the loss experienced by a signal as it travels over long distances, there are still some very rapid fluctuations that occur over very short distances or during short time intervals. Small-scale fading is the name given to these rapid fluctuations in received signal power. The four main factors that influence small-scale fading are multipath propagation, relative motion between the receiver and transmitter, relative motion of objects between the receiver and the transmitter, and the relationship between the signal bandwidth and the bandwidth of the channel [7].

Multipath refers to the fact that a signal sent out from a transmitter will encounter many objects that will reflect and/or scatter the signal in various directions. This results in many copies of the original signal reaching the receiver. The different copies will arrive at the receiver at different times, with different signal strengths and phases. When the received signal is composed of many reflected signals and one line-of-sight signal, the envelope of the signal due to fading has a Rician probability density function. When the line-of-sight, or specular, component is not there then the pdf of the received envelope is Rayleigh distributed.

In this thesis small-scale fading will always be assumed to be Rayleigh distributed. This is because the Rayleigh pdf is more mathematically tractable than the Rician pdf and also because Rayleigh fading represents the worst case fading for the purposes of system design. The distribution of the envelope of a Rayleigh faded signal is expressed as

$$p(r) = \begin{cases} \dfrac{r}{\sigma^2}\exp\left(-\dfrac{r^2}{2\sigma^2}\right) & for\ \ r \geq 0 \\ 0 & otherwise \end{cases} \tag{2.1}$$

where r is the amplitude of the envelope of the received signal, and $2\sigma^2$ is the pre-detection mean power of the multipath signal. The pdf of several Rayleigh random variables with various values of σ is shown in Figure 2.2.

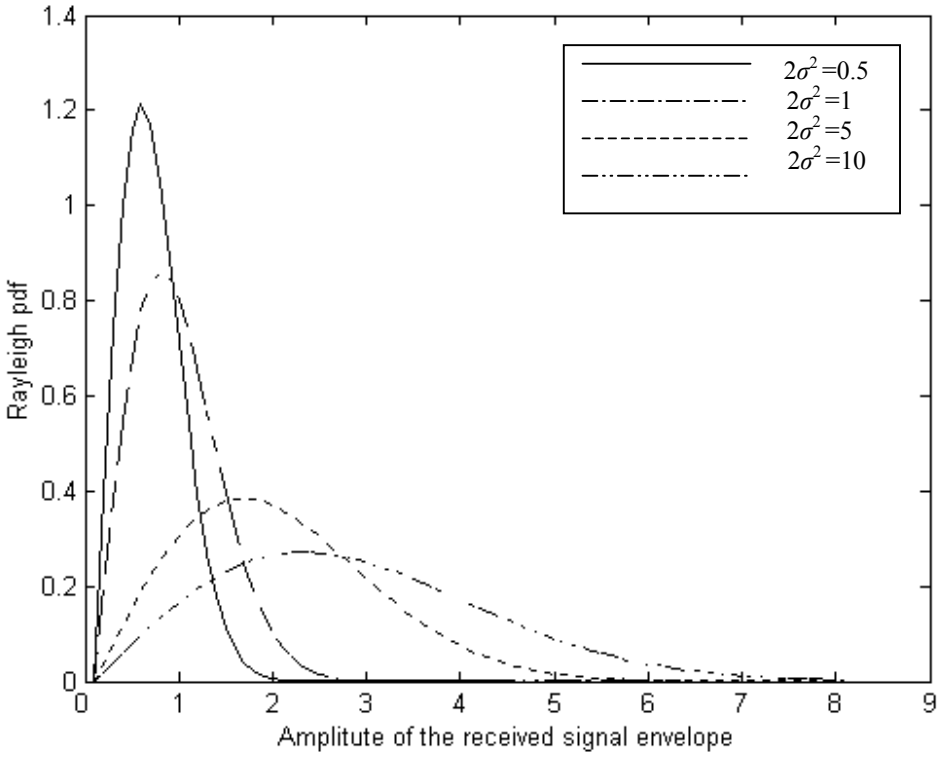

Figure 2.2 Distribution of a Rayleigh random variable

2.2.1 Impulse Response Model

The wireless channel can be modeled as a filter with a time varying impulse response. This impulse response contains all the necessary information needed to account for the small-scale propagation effects. This model can be broken down into two distinct channel characteristics, the time-varying nature and the time-dispersive nature of the channel. The impulse response of a wireless channel can be shown to be

$$h(t,\tau) = \sum_{i=0}^{N-1} a_i(t) \exp\{j(2\pi f_c \tau_i(t) + \phi_i(t))\} \delta(\tau - \tau_i(t)) \tag{2.2}$$

if we express

$$\theta_i(t) = (2\pi f_c \tau_i(t) + \phi_i(t))$$

and

$$\alpha_i(t) = a_i(t)\exp\{j\theta_i(t)\}$$

then

$$h(t,\tau) = \sum_{i=0}^{N-1} \alpha_i(t)\delta(\tau - \tau_i(t)). \tag{2.3}$$

In the above equation $a_i(t)$ represents the variation in the envelope of the signal and is a Rayleigh random variable, $\theta_i(t)$ is a uniform variable representing phase changes, and $a_i(t)$ is a complex Gaussian random variable.

2.2.2 Time Dispersive Nature of the Wireless Channel

In order to examine the time-dispersive nature of the wireless channel we first assume that the impulse response is time-invariant. The impulse response is no longer a function of time and can be represented as

$$\begin{aligned} h(t,\tau) &= h(\tau), \\ h(\tau) &= \sum_{i=0}^{N-1} \alpha_i \delta(\tau - \tau_i). \end{aligned} \tag{2.4}$$

Since it is fairly difficult to measure the impulse response *h(τ),* a more commonly used measure is the power delay profile, or $|h(\tau)|^2$ given as,

$$\left|h(\tau)\right|^2 = \sum_{i=0}^{N-1} a_i^{\,2}\delta(\tau - \tau_i). \tag{2.5}$$

The channel model is normalized so that the initial delay, τ_0 , is equal to zero. Any delay that occurs after the arrival of the first component is referred to as excess delay. The following parameters are used to describe the behavior of the time-dispersive channel: maximum excess delay, mean excess delay, and RMS delay spread. The maximum excess delay corresponds to the delay associated with the last arriving signal component, or $\tau_{N-1} - \tau_0$. Mean excess delay is equivalent to the normalized first moment of the power delay profile. In equation form this is:

$$\bar{\tau} = \frac{\int_{-\infty}^{\infty} \tau |h(\tau)|^2 \, dt}{\int_{-\infty}^{\infty} |h(\tau)|^2 \, dt} = \frac{\sum_{t=1}^{N-1} a_i^{\,2} \tau_i}{\sum_{t=1}^{N-1} a_i^{\,2}}. \tag{2.6}$$

To calculate the RMS delay spread, first take the normalized second moment of the power delay profile

$$\overline{\tau^2} = \frac{\int_{-\infty}^{\infty} \tau^2 |h(\tau)|^2 \, dt}{\int_{-\infty}^{\infty} |h(\tau)|^2 \, dt} = \frac{\sum_{i=1}^{N-1} a_i^{\,2} \tau_i^{\,2}}{\sum_{i=0}^{N-1} a_i^{\,2}}, \tag{2.7}$$

then use this value, $\overline{\tau^2}$, along with the normalized first moment, $\bar{\tau}$, to find the RMS delay spread

$$\sigma_\tau = \sqrt{\overline{\tau^2} - (\bar{\tau})^2} \, . \tag{2.8}$$

All of the parameters dealt with thus far are in the time domain and determine whether or not the wireless channel is time-dispersive. In the frequency domain the channel is said to exhibit frequency-non-selective, also called flat, or frequency-selective fading. The term coherence bandwidth refers to the effective bandwidth of the channel that affects a signal in a similar fashion. In other words the fading is relatively constant over a certain band of frequencies. If the entire frequency content, or bandwidth, of the transmitted signal falls within the coherence bandwidth of the channel then all the frequency components of the signal are effected in the same fashion. This is referred to as flat fading. On the other hand, if the bandwidth of the transmitted signal is larger than the coherence bandwidth of the channel then different frequency components will experience various levels of fading. A channel that acts in this way is known as a frequency-selective channel.

The coherence bandwidth can be calculated from the RMS delay spread. Depending on the assumption of how correlated the fading should be, fifty percent or ninety percent correlation, there are two equations for coherence bandwidth [7]. The two equations are shown below:

$$\text{50\% correlated: } B_c \approx \frac{1}{5\sigma_\tau},$$

$$\text{90\% correlated: } B_c \approx \frac{1}{50\sigma_\tau}.$$

If B_s is the bandwidth of the transmitted signal and B_c is the coherence bandwidth of the channel, then figure 2.3 shows the different cases of fading.

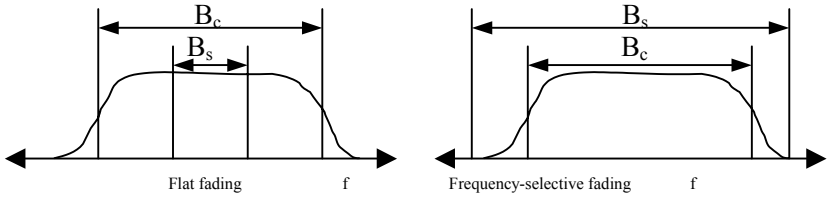

Figure 2.3 Representation of flat or frequency-selective fading

2.2.3 Time Varying Nature of the Wireless Channel

In the previous section the channel was assumed to be time-invariant in order to examine the time-dispersive nature of the channel. In this section we will assume that all the signal components arrive at the same moment rather than as a series multipath components. The impulse response is no longer a sum of components arriving with variable delays, rather it is a single function of time and can be represented as

$$h(t,\tau) = \alpha(t)\delta(\tau)\,. \tag{2.9}$$

This is valid if we assume that

$$\sigma_\tau = T_s$$

where T_s is the transmitted symbol period and σ_τ is the RMS delay spread.

In order to understand the time varying parameters of the channel it is necessary to look at the Doppler shift and how it is calculated. Assume that a base station, located at some point *z*, is broadcasting a signal to a mobile station that is moving from point x to point y with a constant velocity *v*. This situation is depicted in Figure 2.4 below.

The first step is to calculate the path length difference between L_1 and L_2. This difference is labeled as Δl. The Doppler frequency, f_d, will now be found using the information in Figure 2.4 below.

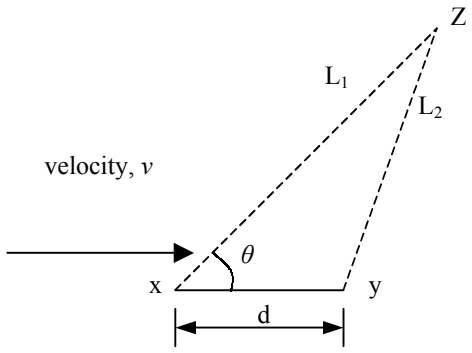

Figure 2.4 Physical description of relative motion between a transmitter and receiver

$$\Delta l = \left| L_1 - L_2 \right| \quad , \quad \Delta l = d\cos(\theta) \tag{2.10}$$

where distance

$$\begin{aligned} d &= v\Delta t \quad , \quad \Delta l = v\Delta t\cos(\theta) \\ \Delta\phi &= \frac{2\pi\Delta l}{\lambda} \quad , \quad \Delta\phi = \frac{2\pi v\Delta t\cos(\theta)}{\lambda} \end{aligned} \tag{2.11}$$

Now calculate the angular frequency measured in radians per second using

$$\omega_d = \frac{\Delta\phi}{\Delta t} \quad , \quad \omega_d = \frac{2\pi v\cos(\theta)}{\lambda} \tag{2.12}$$

Then, the Doppler frequency in hertz is

$$f_d = \frac{\omega_d}{2\pi} \quad , \quad f_d = \frac{v\cos(\theta)}{\lambda}. \tag{2.13}$$

When the mobile channel exhibits a time varying nature the result is a widening of the spectral content of a transmitted signal. The amount of widening, or spreading, is dependent on the Doppler frequency. The Doppler spread, B_D , is the parameter used to describe this broadening of frequency content and is described by

$$B_D = 2f_d \tag{2.14}$$

The maximum Doppler frequency occurs when $\left|\cos(\theta)\right|$ is equal to one and is shown to be

$$f_{d\max} = \pm\frac{v}{\lambda}. \tag{2.15}$$

Coherence time, T_c , is another parameters used to characterize the time varying nature of the channel. It is essentially a statistical measure of the time over which the impulse

response of the channel does not vary. In essence, this means that if two signals are received within a time that is less than the coherence time then those signal amplitudes will be highly correlated. The coherence time is inversely proportional to the Doppler spread leading to the relationship

$$T_c \approx \frac{1}{f_{d\max}}. \tag{2.16}$$

If the coherence time is defined to be the interval over which the correlation of two signals in time is greater than 0.5 then

$$T_c \approx \frac{9}{16\pi f_{d\max}} \tag{2.17}$$

A commonly used method for determining coherence time is to take the geometric mean of equations 2.5 and 2.6 [7] to arrive at

$$T_c = \sqrt{\frac{9}{16\pi f_{d\max}^2}} \quad , \quad T_c = \frac{0.423}{f_{d\max}}. \tag{2.18}$$

2.3 Multiple Input Multiple Output (MIMO) Channels

In the previous sections we have only considered channels with a single input and a single output. In order to analyze or discuss diversity techniques that involve the use of multiple antennas it is necessary to first understand the multiple input multiple output (MIMO) channel model. We discuss diversity techniques in more detail later. Figure 2.5 represents the basic layout of a MIMO channel model. The major difference between the representations of the single input-single output, or SISO channel, and the MIMO channel is the use of vector or matrix notation. In the MIMO channel we no longer have a single input, rather, we have a vector of **M** input signals. At the output there is a vector of **N** output signals. To take into account the fading coefficients between transmit and receive antenna pairs it is necessary to use an **M**×**N** matrix, where $a_{m,n}$ is the complex fading gain between transmit antenna m and receive antenna n. The last component to consider is the noise process, which in this case is also a vector. The noise is represented as a vector of N components, each of which is a sample of additive white Gaussian noise (AWGN).

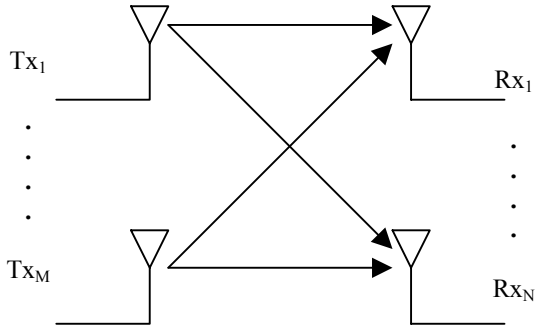

Figure 2.5 Generic model for a MIMO channel

The following shows the design of the input vector **s** , output vector **r** , noise vector **n**, and the fading coefficient matrix **H**. The output is related to the input and the channel parameters by the equation

$$\mathbf{r} = \mathbf{sH} + \mathbf{n} \tag{2.20}$$

where the signal vector, the channel matrix, noise, received vector are given as

$$\begin{aligned} \mathbf{r} &= [r_1 \;\; r_2 \;\; \ldots \;\; r_M], \\ \mathbf{s} &= [s_1 \;\; s_2 \;\; \ldots \;\; s_N], \\ \mathbf{n} &= [n_1 \;\; n_2 \;\; \ldots \;\; n_M], \\ \mathbf{H} &= \begin{bmatrix} \alpha_{11} & \alpha_{12} & \ldots & \alpha_{1M} \\ \alpha_{21} & \alpha_{22} & \ldots & \alpha_{2M} \\ \vdots & \vdots & & \vdots \\ \alpha_{N1} & \alpha_{N2} & \ldots & \alpha_{NM} \end{bmatrix}, \end{aligned} \tag{2.21}$$

respectively.

CHAPTER 3

FUNDAMENTALS OF SPREAD SPECTRUM SYSTEMS

3.1. Spread Spectrum Concept

The traditional approach to digital communications is based on the idea of transmitting as much information as possible in as narrow a frequency bandwidth as possible. Therefore, a concept called narrowband signal s_n is used to yield narrowband systems. The most general concept of spread spectrum systems is presented in Figure 3.1.

Formally, the operation of both transmitter and receiver can be partitioned into two steps. In the first step, which we refer to as primary modulation, the narrowband signal s_n is formed. In the second step, or secondary modulation, the operation $\in(.)$ is applied, resulting in the expansion of the signal spectrum to a very wide frequency band. This signal will be denoted s_w.

At the receiver site, the first step is despreading, which is formally presented by the operation $\in^{-1}(.)=\in(.)$. In other words, after despreading (which is identical to the spreading process) the wideband signal s_w is converted back to the original form s_n and standard methods for narrowband signal demodulation are used. The reasons for doing this are explaining in the next subtitles.

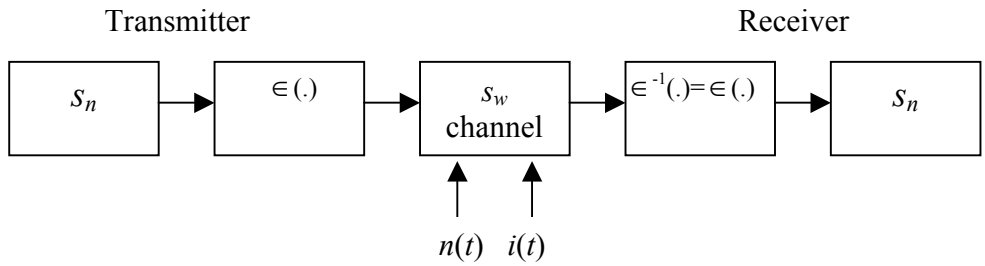

Figure 3.1 Spread spectrum system concept.

3.1.1 Antijamming Capabilities

More than a half of century ago the spread spectrum concept was introduced to solve the problem of reliable communications in the presence of intensive jamming. If we assume that a signal s_w is received in the presence of a relatively narrowband and a much stronger jamming signal $i_n(t)$, then in the despreading process we have

$$\in^{-1}(s_w + i_n) = \in^{-1}(\in(s_n)) + \in^{-1}(i_n) = s_n + i_w \tag{3.1}$$

In other words, the despreading process has converted the input signal into a sum of the narrowband useful and the wideband interfering signals. After narrowband filtering (operation $F(.)$) with the band pass filter of bandwidth B_n equal to the bandwidth of s_n , we have

$$F(s_n + i_w) = s_n + F(i_w) = s_n + i_{wr} \tag{3.2}$$

Only a small portion of the interfering signal energy will pass the filter and remain as residual interference i_{wr} because the bandwidth B_w of i_w is much larger than B_n Figure 3.2 is a schematic representation of the process. One can see from the figure that the power of the residual interference, $P(i_{wr}) = \eta_i B_n$, is related to the overall power of the interference signal, $P(i_{wr}) = \eta_i B_n$, as

$$P(i_{wr}) = \frac{B_n}{B_w} P(i_w) = \frac{1}{G} P(i_w) \quad . \tag{3.3}$$

The parameter

$$G = \frac{B_w}{B_n} \tag{3.4}$$

that shows how much the interfering signal is suppressed in this process, is called the processing gain. We will see later that for different implementations of the system, the statistics of i_{wr} will be different. The antijamming capability of spread spectrum systems has been exploited in military systems for a long time. The evolution of the practical solutions has been very dependent on available technology, and a comprehensive survey of the history of these systems can be found as an introduction to a number of books [1], [9], [10].

If the level of the interfering signal is too high, preliminary processing can be used to suppress interference prior to the $\in^{-1}(.)$ operation. These algorithms use different approaches, but the final effect is the same. A narrow notch in the frequency band occupied by the interference signal is formed using an adaptive algorithm that will be able to follow changes in the interfering signal parameters.

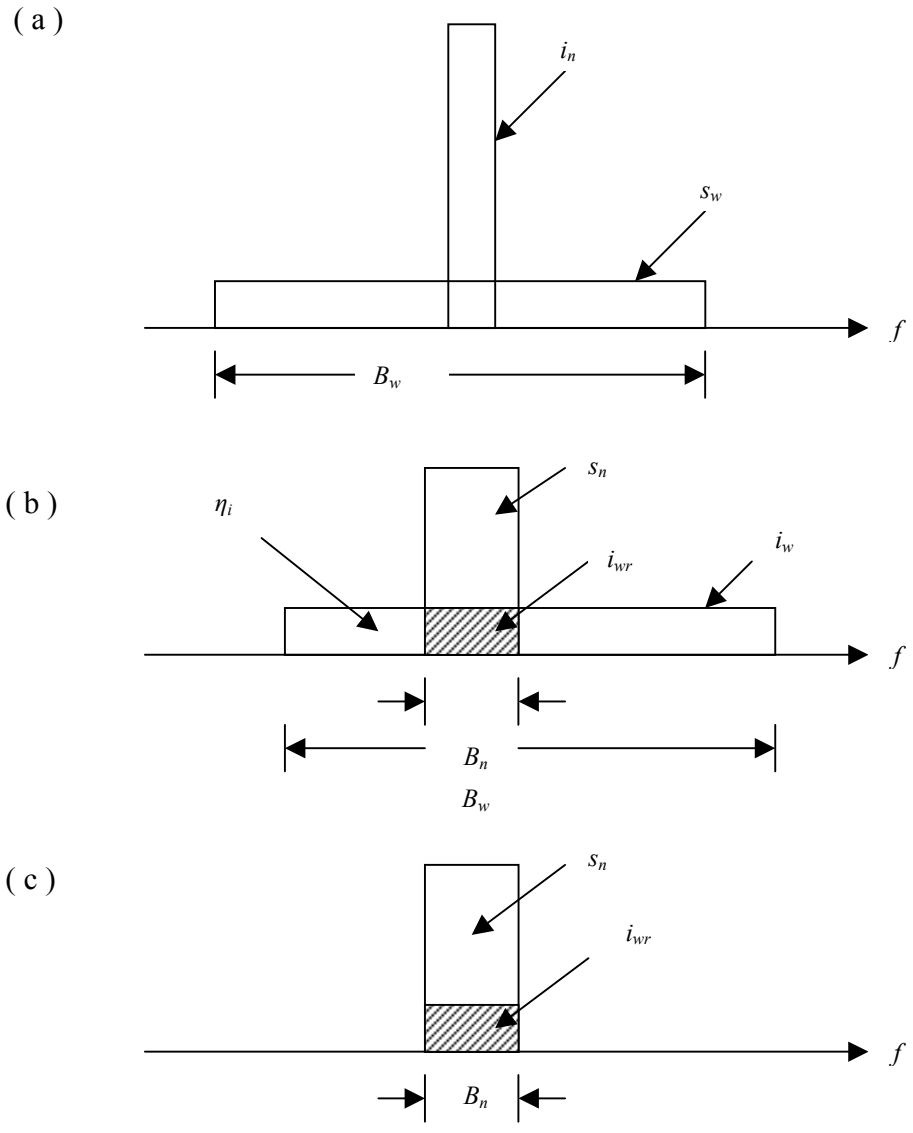

Figure 3.2 Despreading process in the presence of interference : (a) received signal, (b) result of $\in^{-1}(.)$ operation, and (c) result of $F(.)$ operation.

By forming the notch to suppress the interfering signals, a part of the useful signal in the same frequency band will also be removed.

This approach has been used in civil applications too, for so-called code division multiple access (CDMA) overlay type networks. In these networks spread spectrum signals are used in the same frequency band where standard (narrowband) type users already exist. These users with much higher levels are suppressed with both preliminary suppression and spread spectrum processing so that their level in the spread spectrum receiver is tolerable. At the same time, the low spread spectrum signal density produces no excessive interference in the standard narrowband receivers.

3.1.2 Multipath Environment

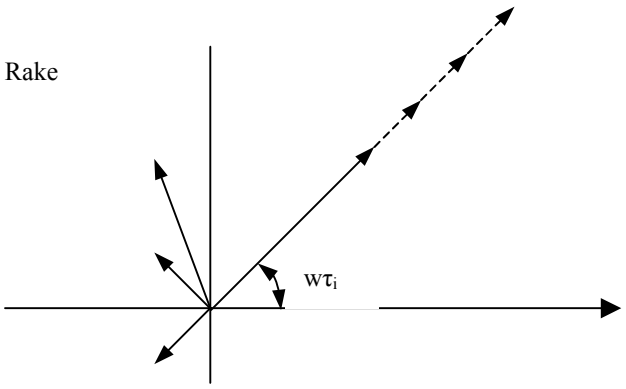

Figure 3.3 Multipath propagation.

As a result of multipath propagation, a transmitted signal will be received as a number of its mutually delayed replicas. A possible phasor representation is given in Figure 3.3. Most of the time, these signal components will act as interference to each other and the net result will be the degradation of the system performance. These components can be separated and combined synchronously into one large signal vector that would provide good signal demodulation conditions. The spread spectrum concept is the so-called Rake-receiver, which will be discussed in more detail later. For now, using previously introduced notation, we can represent the received signal as

$$r(t) = \sum_{l=0}^{L-1} a_l s_w(\tau_l) = \sum_{l=0}^{L-1} a_l \in_{\tau_l} (s_n(\tau_l)) \tag{3.5}$$

where $\tau_0 = 0$ and τ_l is the relative delay (excess delay) experienced by the signal propagating through path l with respect to the signal propagation through the shortest path and a_l is the intensity coefficient of the corresponding path. Most of the time, this coefficient is modeled as a complex, zero mean Gaussian variable. In the receiver, the despreading operation $\in_{\tau s}^{-1}(.) = \in_{\tau s}(.)$, synchronized to the signal with delay τ_s **,** will produce

$$\in_{\tau_s} (r) = \sum_{l=0}^{L-1} \in_{\tau_s} \left[a_l \in_{\tau_l} \left(s_n(\tau_l) \right) \right] \tag{3.6}$$

The signal components will depend only on τ_s - τ_l , which can be represented as $\in_{s-l}$ resulting in

$$\in_{\tau_s} (r) = \sum_{l=1}^{L-1} a_l \in_{s-l} \left[s_n(\tau_l) \right] \tag{3.7}$$

This will result in

$$\in_{s-l} \left[s_n(\tau_l) \right] \Rightarrow \begin{cases} s_n(\tau_l) & if \quad \tau_s - \tau_l = 0 \\ s_n(\tau_l) & if \quad \tau_l - \tau_l > \tau_r \end{cases} \tag{3.8}$$

where τ_r is the range of $\in(.)$ operation. In other words, if the despreading operation is synchronized to the m-th signal component ($\tau_s - \tau_m \cong 0$) and $\tau_s - \tau_l > \tau_r$ after despreading and bandpass filtering, we will have

$$\begin{aligned} F\left\{ \in_{\tau_m} (r) \right\} &= a_m s_n(\tau_m) + \sum_{\substack{l=0 \\ l \neq m}}^{n} a_l s_{wr}(\tau_l) \\ &= a_m s_n(\tau_m) + R_m \end{aligned} \tag{3.9}$$

where $s_{wr}(\tau_l)$ are residuals of the multipath signal components included in R_m. Now if a number of parallel $\in_{\tau i}(.)$ (i = 0, **....** , L - 1) operations are performed, all signal components can be separated and then combined coherently into a signal

$$\sum_{m=0}^{L-1} \left[w_m a_m s_n(\tau_m) + w_m R_m \right] \tag{3.10}$$

where w_m is the combining coefficient. If $a_m\, s_{wr}(\tau_l)$ are independent and if the signal power

is P_s, then the residual R_m will have the power

$$P_{rm} = \frac{P_s}{G} \sum_{\substack{l=0 \\ l \neq m}}^{L-1} |a_l|^2 . \tag{3.11}$$

It can be shown that for the maximum signal-to-noise ratio at the output of the combiner (maximum ratio combining), $w_m \cong a_m^*$. In order to get an initial insight into the system performance we will assume equal gain combining $w_m = 1$ and multipath propagation with $a_l = a$ so that

$$P_{rm} = P_s (L-1) |a|^2 / G . \tag{3.12}$$

Therefore, the signal-to-multipath noise ratio at the output of the combiner with L branches can be approximated as

$$SNR_L = \frac{P_s L^2 |a|^2}{L P_{rm}} = \frac{L^2 G}{L(L-1)} \cong G \qquad L \gg 1 \tag{3.13}$$

If only one signal component is demodulated, we will have

$$SNR_1 = P_s a^2 / P_{rm} = G/(L-1) . \tag{3.14}$$

Of course, this should be considered only as a rough indication of the line of reasoning in using multipath diversity combining in spread spectrum receiver.

3.1.3 Code Division Multiple Access

In order to use bandwidth efficiently, a number of different spread spectrum signals should coexist in the same frequency band. The case when each receiver receives a sum of the signals can be represented as

$$\sum_k s_{wk} = \sum_k \in_k (s_{nk}) \tag{3.15}$$

where index k corresponds to the k-th user in the same frequency band and $\in_k (.)$ defines the spreading operation of user k. In order to be able to coexist, the $\in$ (.) operation should meet the subsequently defined additional requirement. Let us consider the despreading of signal s_{wj} in receiver i.

$$\in_i^{-1}(s_{wj}) = \in_i(\in_j(s_{nj})) = \in_{ij}(s_{nj}) = \begin{cases} s_{nj} & i = j \\ s_{wij} & i \neq j \end{cases} \tag{3.16}$$

In other words, the despreading operation will produce the narrowband signal as long as $i=j$ and the wideband signal s_{wij} as long as $i \neq j$. After bandpass filtering we have

$$F(\in_{ij}(s_{nj})) = \begin{cases} s_{nj} & i = j \\ s_{rij} & i \neq j \end{cases} \tag{3.17}$$

which means that the $F(\in^{-1}(.))$ operation will reproduce the original signal for $i = j$ and will produce only low-level interference s_{wij} for $i \neq j$. As in the previous cases, the power of s_{rij} is less than the power of s_{wij}. So, one despreading of signal in the presence of $K-1$ other signals belonging to different users results in

$$\in_i^{-1}(\sum_k s_{wk}) = s_{ni} + \sum_{\substack{k=1 \\ k \neq i}}^{K} s_{wik} \tag{3.18}$$

or

$$F(\in_i^{-1}(\sum_k s_{wk})) = s_{ni} + \sum_{\substack{k=1 \\ k \neq i}}^{K} s_{rik} \tag{3.19}$$

Hence, mutual separation of the signals is based on a low correlation between operations $\in_i$ and $\in_k$ for $i \neq k$. $\in$ (.) operations are controlled with different codes, hence the name code division multiple access.

3.1.4 Capacity of a CDMA Network

Now suppose that we have K signals of the same power P_s present in the same frequency band. At the input of any receiver signal-to-noise ratio (SNR) is

$$y = P_s/(K-1)P_s = 1/(K-1) \tag{3.20}$$

where the presence of Gaussian thermal noise has been ignored for the moment. After despreading each interfering component coming from another user, which will be suppressed by factor *G,* the SNR becomes

$$y_b = Gy = \frac{G}{K-1}. \tag{3.21}$$

If the thermal noise power is α, then

$$y_b = \frac{P_s G}{P_s(K-1)+\alpha} \tag{3.22}$$

and the system capacity becomes

$$K = 1 + G/y_b - \alpha/P_s \cong G/y_b \tag{3.23}$$

where y_b is the SNR required for the given bit error rate in the system. The system capacity depends on the level of interference that can be tolerated, hence the name interference-limited system. In order to reduce y_b as much as possible, powerful error correcting coding is used.

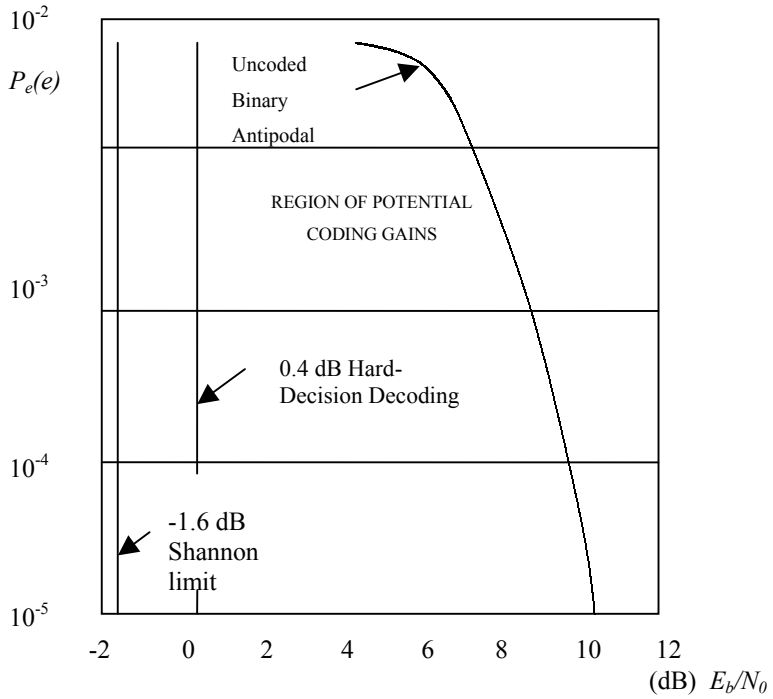

Figure 3.4 Potential coding gains of coded transmission with respect to binary uncoded antipodal transmission. (From: Digital transmission Theory by S. Benedetto, E. Biglieri, and V. Castellani (Prentice Hall, 1987).)

3.2 Examples of Spread Spectrum Systems

3.2.1 Direct Sequence Spread Spectrum System (DSSS)

The most often used form of spreading is obtained if a narrowband PSK signal is directly multiplied by a pseudorandom *(pseudonoise* or PN) sequence, hence the name. Very often the PN sequence is referred to as code, so the notation *c* (code) for the sequence will be used. A PN sequence is an ordered stream of binary ones (+1) and zeros (-1) referred to as chips rather than bits. For an efficient spreading the chip interval T_c is much smaller than the bit interval T_b. So, if the primary phase shift keying (PSK) modulated signal is represented in the form

$$s_n(t) = b(t)\cos\omega_0 t \tag{3.24}$$

then $\in$ (.) represents multiplication of the PSK signal with code $c(t)$. It can be represented as

$$s_w(t) = \in\left(s_n(t)\right) = c(t)s_n(t) = c(t)b(t)\cos\omega_0 t \tag{3.25}$$

The bandwidth of $s_w(t)$ is determined by $c(t)$ and is much higher than the bandwidth of $s_n(t)$ because $1/T_c >> 1/T_b$. $\in^{-1}$ (.) = $\in$ (.) so again the despreading operation is a multiplication by code $c(t)$. This time $s_w(t)$ is multiplied by the code and yields

$$\in^{-1}\left(s_w(t)\right) = c(t)s_n(t) = c(t)s_w(t) = c^2(t)b(t)\cos\omega_0 t = b(t)\cos\omega_0 t = s_n(t) \tag{3.26}$$

From the definition of the $\in$ (.) operation, one can see that for multipath separation $c(t)\cdot c(t-\tau)$ should remain wideband for $\tau > T_s$ (separation interval) and for multiple access capability $c_i(t)\cdot c_j(t-\tau)$ should remain wideband for all *i, j,* and τ. A direct extension to *quadrature* PSK (QPSK) format can be obtained as

$$s_w(t) = c_1(t)b_1(t)\cos\omega_0 t - c_2(t)b_2(t)\sin\omega_0 t$$

where $c_1(t)$ and $c_2(t)$ are two different PN sequences and $b_1(t)$ and $b_2(t)$ two independent data streams. The complex representation of this signal is

$$s_w(t) = \mathrm{Re}\left\{d(t)\exp(jw_0 t)\right\} \tag{3.26a}$$

where

$$d(t) = d_r(t) + jd_i(t) = c_1(t)b_1(t) + jc_2(t)b_2(t)$$

In Figures 3.5 and 3.6 *binary* PSK(BPSK)/DSSS and QPSK/DSSS systems are presented as illustrations. In practice product $c(t)b(t)$ in (3.25) can have additional components. For example, in the IS-95 standard, in order to maximize the system capacity $K = G/y_b$ by minimizing the required y_b for a given quality, $b(t)$ is encoded using convolutional codes and additionally modulated using orthogonal modulation with Walsh functions $W(t)$. So the equivalent data has form $[b(t) * g(t)]W(t)$ where $b(t) * g(t)$ stands for the encoded signal. In addition to this PN sequence, IS-95 is composed of two components, long code $lc(t)$, to separate signals coming from different cells and improve randomness, and short code $sc(t)$, called pilot code, to improve synchronization. So in (1.2) the product $c(t)b(t)$ now becomes $lc(t)\ sc(t)[\ b(t)\ *g(t)]\ W(t)$.

The overall signal demodulation process in the BPSK/DS system can be implemented by multiplying the input signal with a corresponding sequence and coherent carrier and then integrating in the bit interval T_b. The equivalent representation of the process is shown in Figure 3.5. So if K coherent signals are simultaneously transmitted (e.g., downlink transmission in cellular network), then the decision variable for the kth receiver can be represented as

$$\begin{aligned} d_k &= \int_0^{T_b} 2c_k \cos\omega_0 t \left[\sum_{i=1}^{K} c_i b_i \cos\omega_0 t \right] dt \\ &= b_k \int_0^{T_b} c_k c_k dt + \sum_{i \neq k} b_i \int_0^{T_b} c_i c_k dt = b_k T_b + \sum b_i \rho_{ik} T_b \end{aligned} \tag{3.27}$$

where ρ_{ik} is the correlation function defined as

$$\rho_{ik} = \frac{1}{T_b} \int_0^{T_b} c_i c_k dt\ . \tag{3.28}$$

The second component in (3.27) is called multiple access interference (MAI) and should be kept as low as possible. One way to take care of it is to design a set of sequences with as low cross correlations as possible.

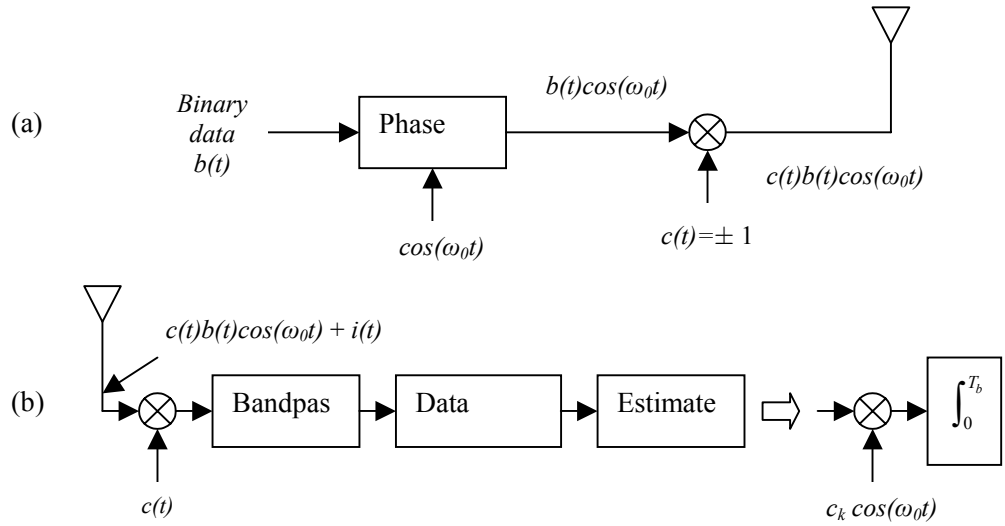

Figure 3.5. PSK direct sequence spread spectrum (a) transmitter and (b) receiver.

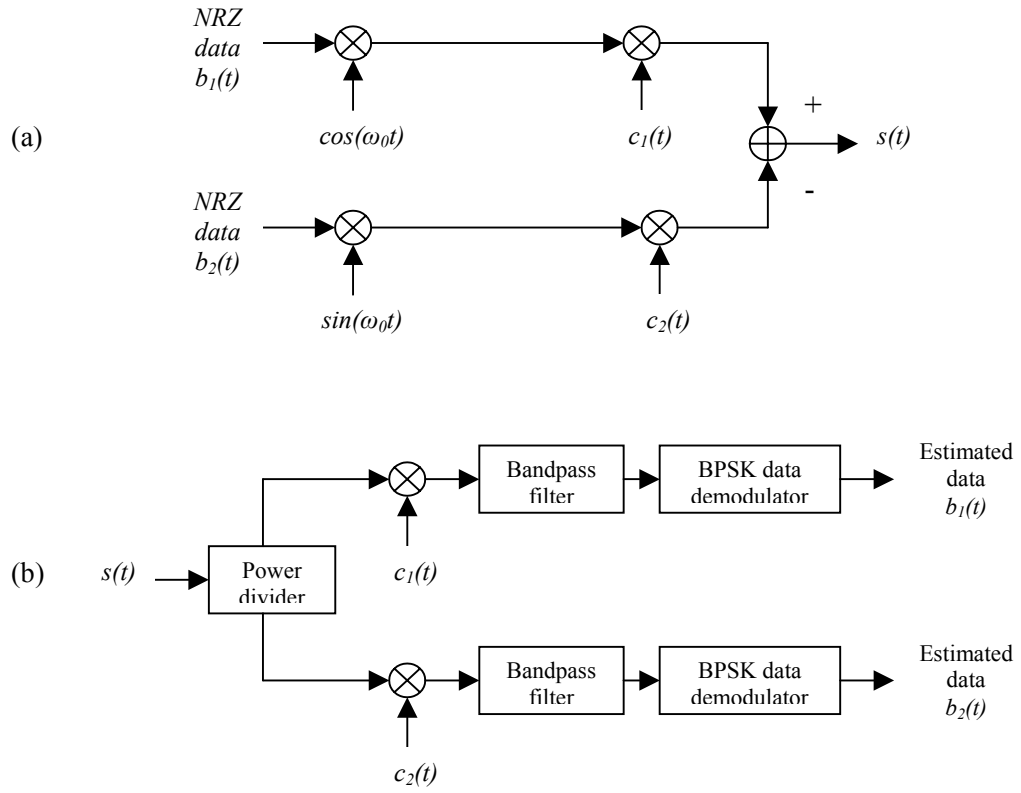

Figure 3.6. QPSK direct sequence spread spectrum (a) transmitter and (b) receiver.

3.2.2 Frequency Hopping Spread Spectrum System (FHSS)

In frequency hopping CDMA, the carrier frequency of the modulated information signal is not constant but changes periodically. During time intervals T the carrier frequency remains the same, but after each time interval the carrier hops to another (or possibly the same) frequency. The hopping pattern is decided by the code signal. The set of available frequencies the carrier can attain is called the *hop-se*t.

The frequency occupation of an FH-SS system differs considerably from a DS-SS system. A DS system occupies the whole frequency band when it transmits, whereas an FH system uses only a small part of the bandwidth when it transmits, but the location of this part differs in time.

The difference between the FH-SS and the DS-SS frequency sage is illustrated in Figure 3.7. Suppose an FH system is transmitting in frequency band 2 during the first time period. A DS system transmitting in the same time period spreads its signal power over the whole frequency band so the power transmitted in frequency band 2 will be much less than that of the FH system. However, the DS system transmits in frequency band 2 during all time periods while the FH system only uses this band part of the time. On average, both systems will transmit the same power in the frequency band.

The data signal is baseband modulated. Using a fast frequency synthesizer that is controlled by the code signal, the carrier frequency is converted up to the transmission frequency. The inverse process takes place at the receiver. Using a locally generated code sequence, the received signal is converted down to the baseband. The data is recovered after (baseband) demodulation. The synchronization/tracking circuit ensures that the hopping of the locally generated carrier synchronizes to the hopping pattern of the received carrier so that correct despreading of the signal is possible.

Within frequency hopping CDMA a distinction is made that is based on the hopping rate of the carrier. If the hopping rate is (much) greater than the symbol rate, one speaks of a fast frequency hopping (F-FH). In this case the carrier frequency changes a number of times during the transmission of one symbol, so that one bit is transmitted in different frequencies. If the hopping rate is (much) smaller than the symbol rate, one speaks of slow

frequency hopping (S-FH). In this case multiple symbols are transmitted at the same frequency.

The occupied bandwidth of the signal on one of the hopping frequencies depends not only on the bandwidth of the information signal but also on the shape of the hopping signal and the hopping frequency. If the hopping frequency is much smaller than the information bandwidth (which is the case in slow frequency hopping), then the information bandwidth is the main factor that decides the occupied bandwidth. If, however, the hopping frequency is much greater than the information bandwidth, the pulse shape of the hopping signal will decide the occupied bandwidth at one hopping frequency. If this pulse shape is very abrupt (resulting in very abrupt frequency changes), the frequency band will be very broad, limiting the number of hop frequencies. If we make sure that the frequency changes are smooth, the frequency band at each hopping frequency will be about $1/T_h$ times the frequency bandwidth, where T_h is equal to the hopping frequency. We can make the frequency changes smooth by decreasing the transmitted power before a frequency hop and increasing it again when the hopping frequency has changed.

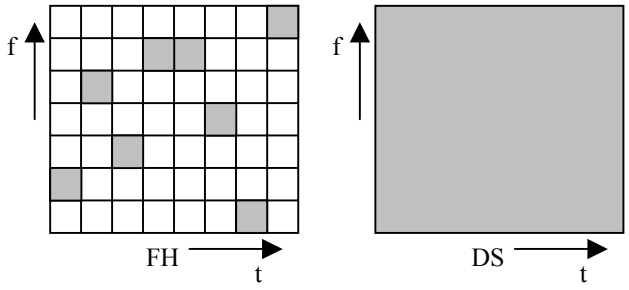

Figure 3.7. Time/frequency occupancy of FH and DS signals.

3.2.3 Time Hopping (TH)

In time hopping CDMA the data signal is transmitted in rapid bursts at time intervals determined by the code assigned to the user. The time axis is divided into frames, and each frame is divided into M time slots. During each frame the user will transmit in one of the M time slots. Which of the M time slots is transmitted depends on the code signal assigned to the user. Since a user transmits all of its data in one, instead of M time slots, the

frequency it needs for its transmission has increased by a factor M. Figure 3.8 shows the time-frequency plot of the TH-CDMA systems. Comparing Figure 3.8 with Figure 3.7, we see that the TH-CDMA uses the whole wideband spectrum for short periods instead of parts of the spectrum all of the time.

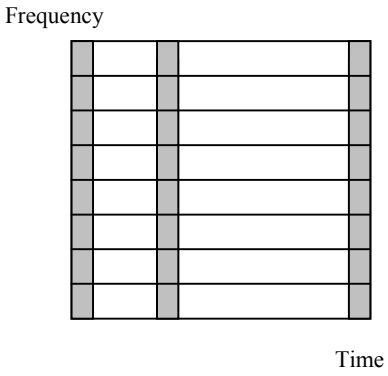

Figure 3.8. Time-frequency plot of the TH-CDMA.

3.2.4 Hybrid Systems

The hybrid CDMA systems include all CDMA systems that employ a combination of two or more of the above-mentioned spread-spectrum modulation techniques or a combination of CDMA with some other multiple access technique. By combining the basic spread-spectrum modulation techniques, we have four possible hybrid systems: DS/FH, DS/TH, FH/TH, and DS/FH/TH; and by combining CDMA with TDMA or multicarrier modulation we get two more: CDMA/TDMA and MC-CDMA.

The idea of the hybrid system is to combine the specific advantages of each of the modulation techniques. If we take, for example, the combined DS/FH system, we have the advantage of the anti-multipath property of the DS system combined with the favorable near-far operation of the FH system. Of course, the disadvantage lies in the increased complexity of the transmitter and receiver.

3.3. Spreading Sequences

The spreading sequences can be classified as orthogonal sequences and pseudonoise (PN) sequences. The cross correlation of the orthogonal sequences is zero and so MAI from other users is cancelled. Orthogonal sequences are used in synchronous CDMA systems because the cross correlation function varies remarkably as a function of the time shift of the sequences.

The pseudonoise (PN) sequences have auto-correlation function that is similar to white Gaussian noise. The received sequences from other users are also noise-like signals. MAI from other users is distributed evenly in time and between the interfering users. This allows asynchronous operation. They are chosen to have three desirable attributes [11]:

1) Each element of the sequence (1,0 or +1, -1) occurs with equal frequency,
2) The auto-correlation has small off-peak values to allow rapid sequence acquisition and
3) Cross-correlation is small at all delays.

However, the attributes 2) and 3) are difficult to achieve simultaneously. Designing the sequences to have low cross correlation reduces the randomness of the sequences and increases the off-peak values of the auto-correlation function [Oja98]. Spreading sequences are often characterized in terms of their discrete-time correlation properties with the time shift n. When short codes are used the auto- and cross-correlation are calculated over a full sequence period N. When they are calculated periodically the values of sequential data symbols are ignored.

The periodic auto-correlation of the k-th complex spreading sequence $c^{(k)}$ over a c full period *N* is [11]

$$\phi_{k,k}(n) = \frac{1}{2N}\sum_{i=0}^{N-1} c_i^{(k)} c_{i+n}^{(k)^*} \tag{3.29}$$

and the periodic cross-correlation over a full period N between the *k*-th and *m*-th sequences $c^{(k)}$ and $c^{(m)}$ is [11]

$$\phi_{k,k}(n) = \frac{1}{2N}\sum_{i=0}^{N-1} c_i^{(k)} c_{i+n}^{(m)^*} \tag{3.30}$$

The aperiodic auto-correlation over the full period N of the sequence $c^{(k)}$ calculates only the overlapping part of the sequences ([11]).

$$\phi^{a}_{k,k}(n)=\begin{cases}\dfrac{1}{2N}\displaystyle\sum_{i=1}^{N-n} c_{i+n}^{(k)}c_i^{(k)^*} & ,\ 0\le n\le N-1\\ \dfrac{1}{2N}\displaystyle\sum_{i=1}^{N-n} c_i^{(k)}c_{i-n}^{(k)^*} & ,\ -N+1\le n\le 0\\ 0 & ,\ |n|\ge N\end{cases} \tag{3.31}$$

Similar equations are obtained for the aperiodic cross-correlation of sequences $c^{(k)}$ and $c^{(m)}$ over a full period N.

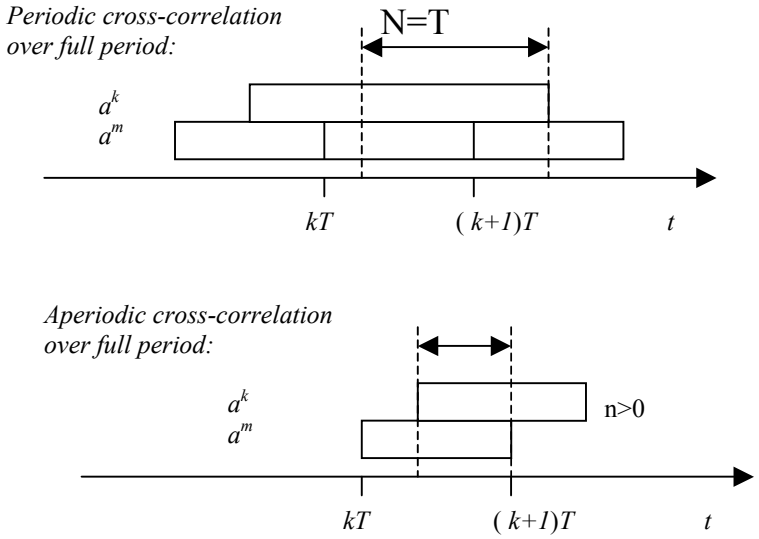

Figure 3.9. Periodic and aperiodic full period auto- and cross-correlations

$$\phi_{k,k}(n)=\phi^{c}_{k,k}(n)+\phi^{c}_{k,k}(n-N) \tag{3.32}$$

By using the aperiodic auto-correlation the effect of different consequent symbols can be taken into account [13]: $\phi_{k,k}(n,b_{-1},b_0)=b_0\cdot\phi^{c}_{k,k}(n)+b_{-1}\cdot\phi^{c}_{k,k}(n-N)$,b_{-1} and b_0 are consequent symbols (+1,-1). When long codes are used the partial period auto- and cross-correlations are calculated over the bit period $T=G\ .T_c$ instead of the whole sequence period N [11].

$$\begin{aligned}\phi^{p}_{k,k}(n)&=\frac{1}{2G}\sum_{i=0}^{G-1}c_i(k)+c_{i+n}{}^{(k)^*}\\ \phi^{p}_{k,p}(n)&=\frac{1}{2G}\sum_{i=0}^{G-1}c_i(k)+c_{i+n}{}^{(m)^*}\end{aligned} \tag{3.33}$$

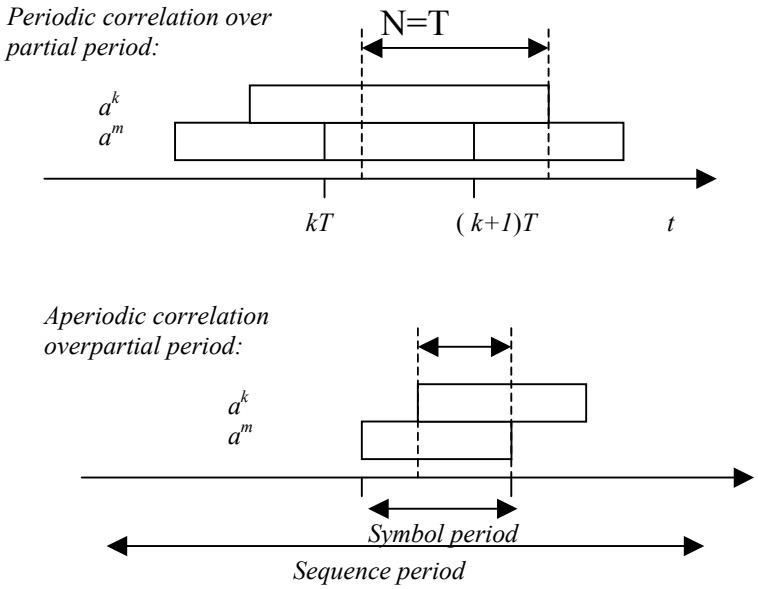

Figure 3.10. Periodic and aperiodic partial period auto- and cross-correlations.

The partial period correlations are not only a function of the delay n, but also depend upon the point in the sequence where the summation actually starts. They are difficult to derive analytically. Therefore, statistical auto- and cross-correlations are used assuming that the sequences with elements {±1,±j} are randomly generated.

The mean and variance of the partial period autocorrelation (periodic) are ([11])

$$\mu_{\phi^p{}_{k,k}}(n) = E[\phi^p{}_{k,k}(n)] = \frac{1}{2G}\sum_{i=1}^{G-1} E[c_i^{(k)}\, c_{i+n}^{(m)^*}] = \delta_{n,lN} = \begin{cases} 1\ , & n = lN \\ 0\ , & n \neq lN \end{cases}$$
$$\sigma^2_{\phi^p{}_{k,k}}(n) = E[\left|\phi^p{}_{k,k}(n)\right|^2] - \mu^2_{\phi^p{}_{k,k}}(n) = (1-\delta_{n,lN})\frac{1}{G} = \begin{cases} 0 & , \ n = lN \\ 1/G & , \ n \neq lN \end{cases} \tag{3.34}$$

The mean and variance of the partial period cross-correlation (periodic) are [11]

$$\mu_{\phi^p{}_{k,k}}(n) = E[\phi^p{}_{k,m}(n)] = 0\ ,\ \forall n$$
$$\sigma^2_{\phi^p{}_{k,k}}(n) = E[\left|\phi^p{}_{k,m}(n)\right|^2] - \mu^2_{\phi^p{}_{k,m}}(n) = 1/G\ ,\ \forall n \tag{3.35}$$

3.3.1. Spreading Waveforms

In asynchronous systems the auto- and cross-correlation for the continuous-time waveforms depend also on the amount of overlapping δ of the chip waveforms :

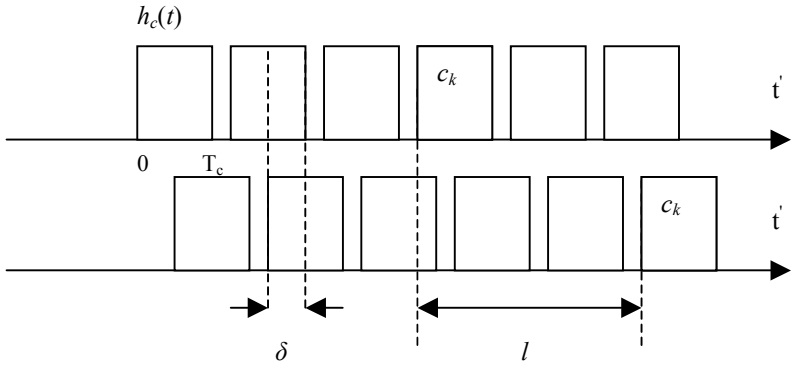

Figure 3.11. Chip overlapping.

The continuous-time periodic cross-correlation over a full period between the spreading waveforms $c^{(k)}(t)$ and $c^{(m)}(t)$ depends both on the time shift between the sequences l (earlier-n) and the chip overlapping time shift δ [11]:

$$R_{k,m}(\tau) = \frac{1}{T}\int_0^T c^{(k)}(t)c^{(m)}(t+\tau)dt \quad , \tau = lT_c + \delta$$
$$= \phi_{k,m}(l)R_h(\delta) + \phi_{k,m}(l+1)\bar{R}_h(\delta) \ , \ R_h(\delta), \bar{R}_h(\delta) : \text{chip waveform correlations} \tag{3.36}$$

For rectangular chip waveform $h_c(t) = u_{T_c}(t)$:

$$R_{k,m}(\tau) = \phi_{k,m}(l)\left(1 - \frac{\delta}{T_c}\right) + \phi_{k,m}(l+1)\frac{\delta}{T_c} \ , \ \tau = lT_c + \delta \tag{3.37}$$

The maximum auto- and cross-correlations are obtained by the chip-synchronous approximation (δ=0) :

$$R_{k,k}(\tau) \le \phi_{k,k}(l) \ , \ R_{k,m}(\tau) \le \phi_{k,m}(l) \tag{3.38}$$

The partial period auto- and cross correlations are statistical funtions.

3.3.2. M-Sequences

A widely used type of PN sequences are the maximum-length shift-register sequences (LFSR), m-sequences. Each sequence is generated by a separate LFSR that has m stages. The period of the sequence (sequence length) is $N = 2^m - 1$. They are the longest sequences that can be generated by an LFSR for a given *m* [11].

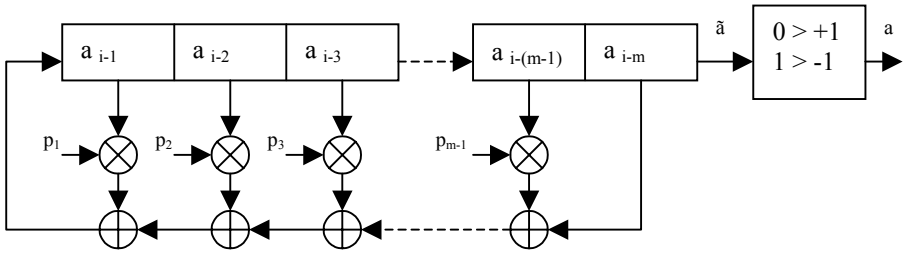

Figure 3.12. M-Sequence generator.

The multipliers $pi \in \{0,1\}$ and $\oplus$ denotes modulo 2 addition . The elements (chips) of the sequence $c_i \in \{0,1\}$ are mapped to $\{+1,-1\}$ for bipolar coding. The sequence *c*(*k*) has 2^{m-1} ones and $2^{m-1}-1$ zeros. The feedback polynomial is a primitive polynomial of degree *m* over GF(2) [11] :

$$P(x) = 1 \oplus p_1 x \oplus p_2 x^2 \oplus p_3 x^3 \oplus \ldots \oplus p_{m-1} x^{m-1} \oplus x^m \tag{3.39}$$

An *m*-sequence has almost an ideal full period autocorrelation:

$$\phi(n) = \begin{cases} 1 & , \ n = lN \\ -1/N & , \ n \neq lN \end{cases} \tag{3. 40}$$

The full period auto-correlation function for continuous time sequence waveforms $c^{(k)}(t)$ when the rectangular chip shaping function $h_c(t) = u_{T_c}(t)$ is used is:

$$R_{k,k}(\tau) = \phi_{k,k}(l)\left(1 - \frac{\delta}{T_c}\right) + \phi_{k,k}(l+1)\frac{\delta}{T_c} \ , \ \tau = lT_c + \delta \tag{3. 41}$$

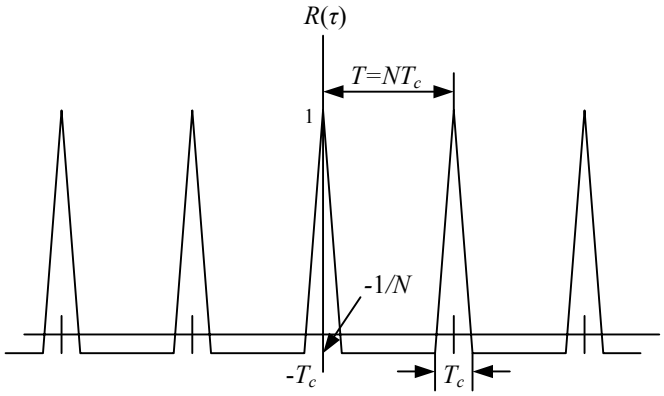

Figure 3.13. Typical full period autocorrelation function of an m-sequence spreading waveform.

However, only for certain values of m there exist some pairs of m-sequences with low full period cross-correlation. When the average full period cross-correlation between sequences $c^{(k)}$ and $c^{(m)}$ is calculated for different shifts n of the sequences:

$$\theta = \frac{1}{N}\sum_{n=0}^{N-1}\phi_{k,m}(n) \tag{3. 42}$$

the value of θ varies much depending on the particular pair of *m*-sequences that are selected and the worst θ-values are great.

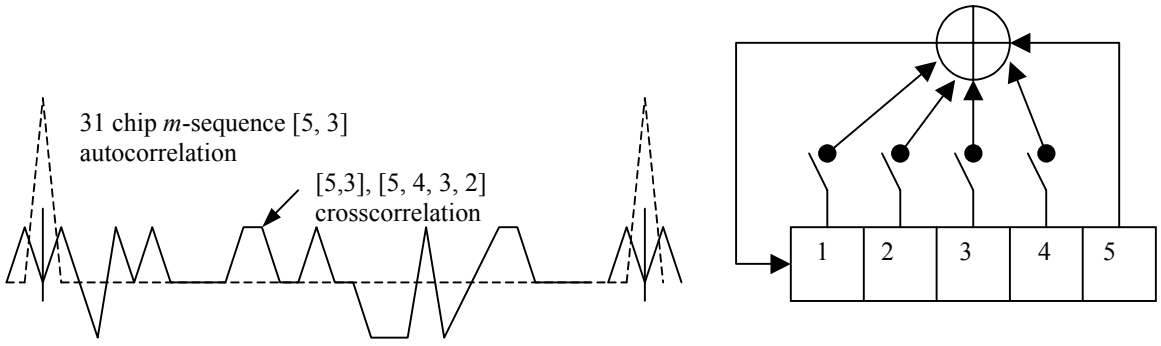

Figure 3.14. Cross-correlation function of typical m-sequences [14].

Table 3.1. Best and worst case average cross-correlations for m-sequences.

M	N	Number of m-sequences	θ Worst	θ Best
5	31	6	0,35	0,29
6	63	6	0,36	0,24
7	127	18	0,32	0,13
8	255	16	0,37	0,12
9	511	48	0,22	0,06
10	1023	60	0,37	0,06
11	2047	176	0,14	0,03
12	4095	144	0,34	0,03

3.3.2. Gold Sequences

A set Gold sequences consist of 2^{m+1} sequences having the period $N = 2^m - 1$ that are generated by a preferred pair of m-sequences. This set contains both the preferred pair ($c^{(1)}$,$c^{(2)}$) and the 2^{m-1} new generated sequences. The sequences are generated by taking a modulo-2 sum of $c^{(1)}$ with the 2^{m-1} cyclically shifted versions of $c^{(2)}$ or vice versa.

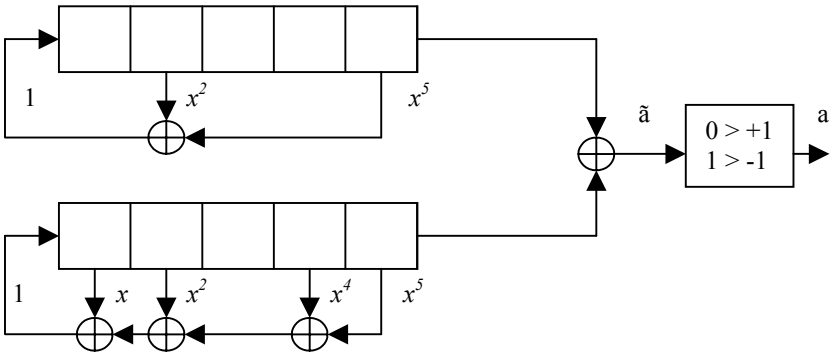

Figure 3.15. A Gold sequence generator with $p_1(x)= 1+x^2+x^5$ and $p_2(x)= 1+x+x^2+x^4+x^5$
This sequence generator can produce 32 Gold sequences of length 31 [11].

Because the Gold sequences are not maximal length sequences (except $c^{(1)}$ and $c^{(2)}$) the auto-correlation function is not 2-valued. Both the cross-correlation and off-peak autocorrelation functions are 3-valued : {-1, -$t(m)$, t(m)-2}, where

$$t(m) = \begin{cases} 2^{(m+1)/2+1} & \text{, when } m \text{ is odd} \\ 2^{(m+2)/2} + 1 & \text{, when } m \text{ is even} \end{cases} \quad (3.43)$$

So both the cross correlation and off-peak auto-correlation functions are upper bounded by $t(m)$:

Table 3.2. Peak cross correlation of m-sequences and Gold-sequences [11].

N	Number M sequences	Peak cross Correlation	m-sequence $\Phi_{max}/\Phi(0)$	t(m)	Gold sequence t(m)/ $\Phi(0)$
7	2	5	0,71	5	0,71
15	2	9	0,60	9	0,60
31	6	11	0,35	9	0,29
63	6	23	0,36	17	0,27
127	18	41	0,32	17	0,13
255	16	95	0,37	33	0,13
511	48	113	0,22	33	0,06
1023	60	383	0,37	65	0,06
2047	176	287	0,14	65	0,03
4095	144	1407	0,34	129	0,03

3.3.3. Kasami Sequences

The small set of Kasami sequences consists $2^{m/2}$ sequences having the period $N = 2^m - 1$. This set is generated in a way similar to the Gold sequences by using a pair of a long sequence $c^{(1)}$ and a short sequence $c^{(2)}$ that are m-sequences. This set contains both the long sequence $c^{(1)}$ and the $2^{m/2} - 1$ new generated sequences. The sequences are generated by taking a modulo-2 sum of $c^{(1)}$ with all the $2^{m/2} - 1$ cyclic shifts of $c^{(2)}$.

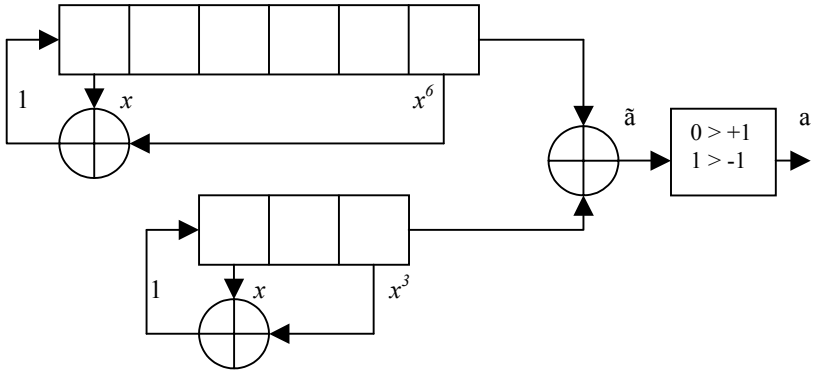

Figure 3.16. A Kasami sequence generator with $p_1(x)= 1+x+x^6$ and $p_2(x)= 1+x+x^3$. This sequence generator can produce 8 Kasami sequences of length 63 [11].

Like for Gold sequences the cross-correlation and off-peak auto-correlation functions are 3valued. The possible values are : {-1, -s (m), s(m)-2}, where $t(m) = 2^{m/2} + 1$

The upper bound $s(m)$ for the cross correlation and off-peak auto-correlation functions is reduced to half compared with the Gold sequences of the same length.

The large set of Kasami sequences contains also Gold sequences and hence the crosscorrelation and off-peak autocorrelation values are on the average higher than in the small set of Kasami sequences.

3.3.4. Barker Sequences

The Barker sequences are aperiodic sequences (finite length sequences). Their crosscorrelation and off-peak auto-correlation values are limited by 1/N but they are known only for code lengths N=2,3,4,5,7,11. Because the Barker sequences are short and their number is limited they are used for special purpose systems (as for initial synchronization and wireless LANs).

a=(+1-1), a=(+1+1-1), a=(+1+1-1+1), a=(+1+1+1-1+1), a=(+1+1+1-1-1+1-1)

a=(+1+1+1-1-1-1+1-1-1+1-1), a=(+1+1+1+1+1-1-1+1+1-1+1-1+1)

$$\phi^{c}_{k,k}(n) = \begin{cases} 1 & , \ n = 0 \\ 0 \ , \ \frac{1}{N} \text{ or } -\frac{1}{N} & , \ n \neq 0 \end{cases} \qquad (3.44)$$

3.3.5. Walsh-Hadamard Sequences

The Walsh-Hadamard sequences are orthogonal sequences. They are the rows of the Hadamard matrix that is obtained by the recursion :

$$H_{2M} = \begin{bmatrix} H_M & H_M \\ H_M & -H_M \end{bmatrix} \text{ starting from } H_2 = \begin{bmatrix} 1 & 1 \\ 1 & -1 \end{bmatrix} \tag{3.45}$$

The Walsh-Hadamard sequences can be used either to spread orthogonally (orthogonal CDMA) the signals of the different users or for M-ary orthogonal coding the different symbols.

If orthogonal sequences are used for different users accurate synchronization is needed because the orthogonal sequences have for non-zero time shifts large cross-correlation and off-peak auto-correlation values.

If orthogonal symbols are used $k=\log_2 M$ bits are used to encode one of the orthogonal symbols. The user signals are spread by different pseudonoise sequences.

3.4. Rake Receiver

In the previous section we showed that wideband signals in a multipath environment are frequency selective. Such channels are described by a tapped delay line model. Since CDMA spreading codes are designed to have very low crosscorrelation between successive chips, multipath components delayed by more than one chip duration are uncorrelated and appear as resolvable paths in the model. Typically, CDMA systems are designed to have several resolvable paths within the multipath delay spread. At the same time, the delay spread is chosen to be lower than the bit duration T. If the delay spread is greater than the bit duration T, then the data rate is higher than the coherence bandwidth, which results in intersymbol interference. To avoid intersymbol interference, the data rate should be maintained below the coherence bandwidth.

When the delay spread is lower than T and there are several delayed versions of the transmitted code sequence with delay differences greater than T_c, they will have a low correlation with the original code sequence. Thus, each of these delayed signals will appear

at the receiver as another uncorrelated user and will be ignored by the matched filter receiver of the desired signal.

However, spread spectrum signals are inherently resistant to multipath fading since multipath components carry the information about the transmitted signal and they are independent. Thus, if one of the multipath components is attenuated by fading, the other may not be and the receiver could use unfaded components to make the decision. The CDMA receiver that takes advantage of the multiple paths to provide diversity is called a Rake receiver.

The Rake receiver, shown in Figure 3.17, consists of a bank of correlators. Each of them is used to detect separately one of the L strongest multipath components. This receiver is basically a diversity receiver based on the fact that the multipath components in a CDMA system are uncorrelated if the relative delays are larger than the chip period.

As in other diversity receivers, the outputs from the correlators are weighted and added to compute the estimate for the transmitted signal. If the maximal ratio combining technique, which gives the highest reduction of fading, is used, the weighting coefficient is the complex conjugate of the corresponding channel tap coefficient

Each multipath demodulator in the Rake receiver is called a *finger*. In the original Rake receiver [15] the delay between consecutive taps and the number of taps was fixed. These receivers required a large number of taps in order to capture major multipath components. Modern receivers have only a few Rake fingers and re capable of adjusting the tap positions.

For the operation of the Rake receiver it is necessary to identify and track major multipath components as well as to estimate their relative delays, amplitudes, and phases. The estimation of these parameters is best performed by transmitting unmodulated signals in the form of periodic preambles or pilot tones [16].

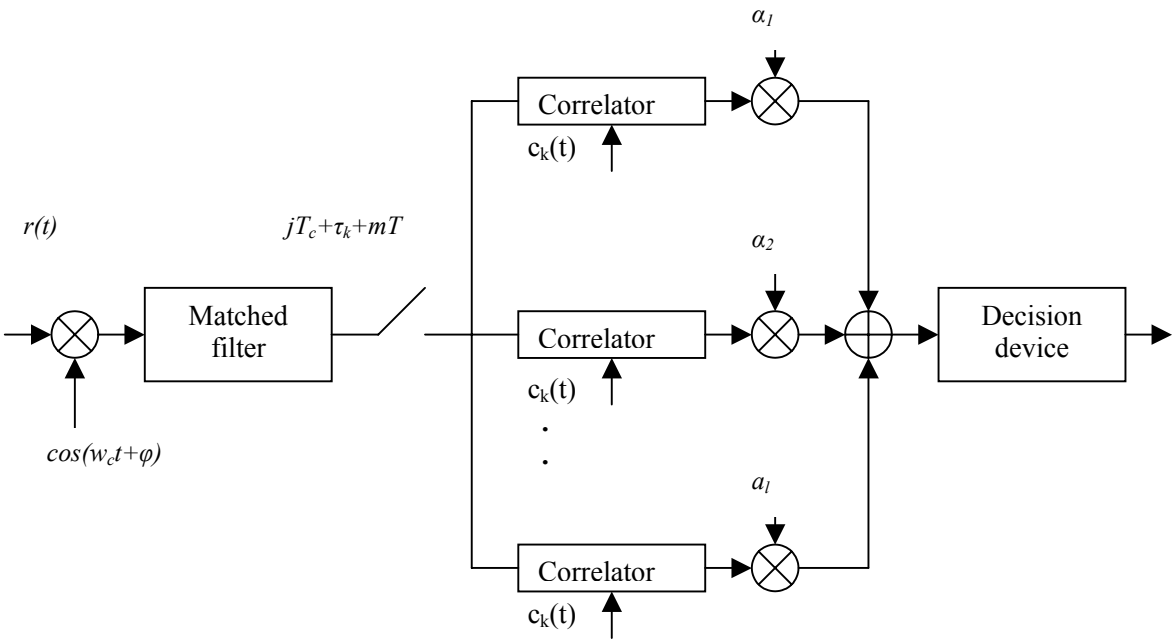

Figure 3.17. A Rake Receiver with L branches.

C H A P T E R 4

SPACE-TIME BLOCK CODES

4.1 Introduction

One of the goals of modern wireless communication systems is to increase the data rates of users without excessive bandwidth expansion. Spectrum is sometimes limited while users continue to demand more data intensive applications, like wireless Internet access, videoconferencing, and streaming multimedia. In order to compensate for the extreme signal degradation that can occur in wireless channels some type of diversity is essential to the functioning of a wireless communication system. It is not uncommon for a wireless system to employ both diversity techniques and channel coding for error detection and/or correction. An effective diversity technique is the use of multiple antennas to provide an improvement in reception without drastically reducing the data rate or increasing the bandwidth. The initial implementations of antenna diversity consisted of using two or more receive antennas. This is a practical technique to use at the base station in a cellular system but not nearly as practical for use in the mobile handsets. If each mobile handset were equipped with multiple receive antennas then the size and cost of each unit would increase beyond what is acceptable to the consumer. If multiple receive antennas cannot be used in the mobiles then diversity gain can only be achieved at the base station.

Research was then being conducted into the feasibility of achieving a suitable diversity gain by using multiple transmitting antennas. A simple scheme for achieving diversity gain without bandwidth expansion using two transmit antennas and any number of receive antennas was devised by S. Alamouti in [3]. Another promising method to provide high data rates, good error performance, and minimal bandwidth expansion is space time coding. Space time coding was introduced in [17] by Tarokh et al. The original space time codes were trellis codes. The codes developed provided maximum diversity gain, dependent on the number of antennas used, and good coding gain, depending on the number of states in the trellis. The complexity of the trellis-based codes is fairly high and increases exponentially with the number of states in the trellis. The performance of trellis

based space-time codes in the presence of channel estimation errors and fading was examined in [18].

It would be desirable to come up with a method to achieve maximum diversity gain but with minimal decoding complexity. Space-time block codes, as introduced in [19], are one such method. Space-time block codes are an extension of the simple scheme developed in [3] to use an arbitrary number of transmit and receive antennas. Space-time block codes utilize a block coding method, as opposed to a trellis-based method, to eliminate much of the processing needed at the receiver. Since the block coding requires only linear processing at the receiver, the decoding can be done efficiently and quickly. Space-time block codes can be constructed for any type of signal constellation and provide full diversity gain at half the maximum possible transmission rate allowed by the theory of space-time coding. For real signal constellations, such as Pulse Amplitude Modulation (PAM), space-time block codes provide the maximum possible transmission rate allowed by the theory of space-time coding.

4.2 General Theory

The transmission model for the space-time block code system is taken from [19] and the rest of this section will define that model. In a space-time block coding system there are *m* transmit antennas and *n* receive antennas. At a given time slot *t*, *m* signals $s_t^i \quad i = 1, 2, ...m,$ are sent simultaneously from the *m* transmit antennas. A block diagram of the transmission side of the system can be seen in Figure 4.1.

The signal received at antenna *j* during time *t* is

$$r_t^i = \sum_{i=0}^{m} a_{i,j}\, s_t^i + n_t^j \tag{4.1}$$

Where $a_{i,j}$, is the path gain between transmit antenna *i* and receive antenna *j*, and n_t^j is the noise at receive antenna *j*. The channel is assumed to undergo flat-fading and the fading is independent between different transmit antennas. The path gains are considered to be independent samples of a complex Gaussian distribution with a variance of 0.5 per real dimension. The noise at the receiver is independent from the path gains and in the form of

additive Gaussian noise with a mean of zero and a variance equal to $n/(2*SNR)$, where m is the number of transmit antennas and SNR is a ratio, not in dB.

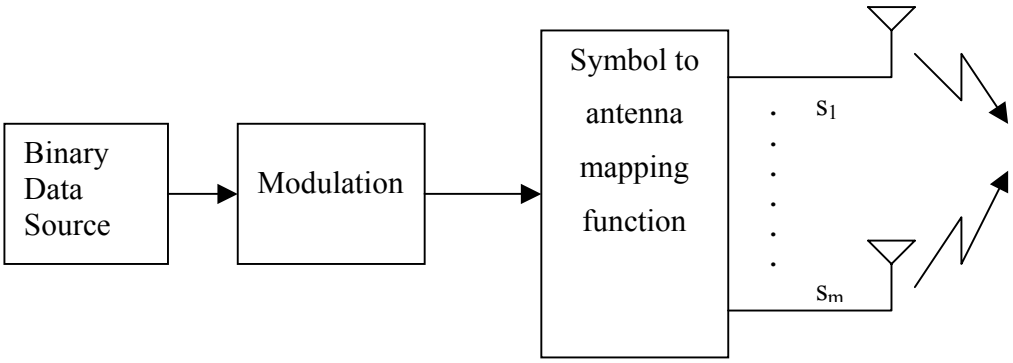

Figure 4.1 Transmission side of Space-Time Block Code system.

The average energy is normalized to be unity for each symbol leaving each of the m transmitting antennas. This gives the energy of the received signal as m and SNR is measured at the receiver. The decoding for this system is rather simple and consists of minimizing the following metric,

$$\sum_{t=1}^{l}\sum_{j=1}^{n}\left|r_t^j - \sum_{i=1}^{m} a_{i,j}\, s_t^i\right|^2 \tag{4.2}$$

over all possible combinations of transmitted symbols. A block diagram of the receiving side of this system can be seen in Figure 4.2.

The encoding process is done based on the data rate the system requires. There is some signal constellation, used for modulation, which maps binary data to real or complex symbols. If there are 2^b symbols in the signal constellation, then k×b bits enters to the modulator at one time slot. These k×b bits will be used to select k symbols that will be sent out over m transmit antennas simultaneously.

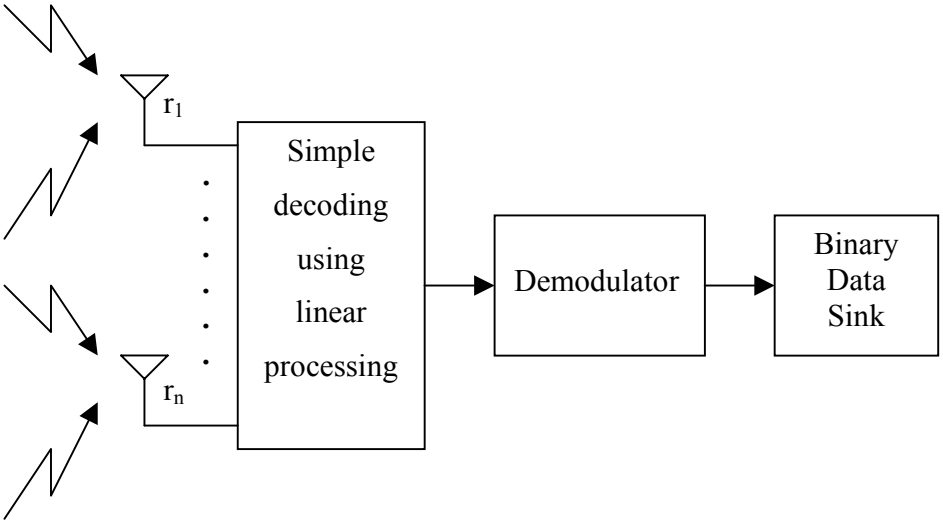

Figure 4.2 Receiving side of Space-Time Block Code system.

The rate of transmission is

$$R = \frac{k}{p} \tag{4.3}$$

where k is the number of symbols that will have to be decoded and p is the number of time slots it takes to transmit all the symbols. The notation denoting the process by which modulation symbols are mapped to different antennas is a simple p×n matrix. An example is the encoder matrix

$$\mathbf{G_2} = \begin{bmatrix} x_2 & x_1 \\ -x_1^* & x_2^* \end{bmatrix}$$

where the i^{th} row determines the symbols transmitted in time slot i, and the j^{th} column determines the symbols transmitted from antenna j over all time slots. Several other encoder matrices were developed in [19].

The decoding of the space time block code is performed by minimizing the metric shown in equation (4.1) above. However, this can be broken down into a simpler form where the metrics can be separated into several equations, each dependent only on a single transmitted symbol. For the specific case of the code defined by $\mathbf{G_2}$, the metric can be decomposed into two simpler equations. Each one needs only to be evaluated over the

possible values that a single symbol can take on, rather than over combinations of symbols. The two equations for this case can be derived as follows:

There are two time slots over which signals will be received at each receive antenna generating two received signals r_1^j and r_2^j . These signals can be shown to be

$$\begin{aligned} r_1^j &= a_{1,j}\, x_2 + a_{2,j}\, x_1 + n_1^j\,, \\ r_2^j &= -a_{1,j}\, x_1^* + a_{2,j}\, x_2^* + n_2^j\,. \end{aligned} \tag{4.4}$$

This can be shown in matrix form to be

$$r^j = \begin{pmatrix} r_1^j \\ (\, r_2^j)^* \end{pmatrix} = \begin{pmatrix} a_{1,j} & a_{2,j} \\ a_{2,j}^* & -a_{1,j}^* \end{pmatrix} \begin{pmatrix} x_2 \\ x_1 \end{pmatrix} + \begin{pmatrix} n_1^j \\ (\, n_2^j)^* \end{pmatrix} \tag{4.5}$$

where, for convenience, we have conjugated the equation for r_2^j so that the signals x_2 and x_1 do not need to be conjugated.

If we take the two received signals as shown in equation (4.4) and substitute into equation (4.2) then we have the new decision metric

$$\sum_{j=1}^{N} \left(\left| r_1 - a_{11} x_2 - a_{21} x_1 \right|^2 + \left| r_2 - a_{11} x_1^* - a_{21} x_2^* \right|^2 \right). \tag{4.6}$$

Next we can use the identity $\left|\xi\right|^2 = \xi \times \xi^*$. To further expand the previous metric into the following two metrics which can be evaluated separately in order to simplify the decoding structure.

$$\left| \left[\sum_{j=1}^{n} (r_1^j a_{1,j}^* + (r_2^j)^* a_{2,j}) \right] - x_2 \right|^2 + \left(-1 + \sum_{j=1}^{n} \sum_{i=1}^{2} \left| a_{i,j} \right|^2 \right) \left| x_2 \right|^2 \tag{4.8}$$

$$\left| \left[\sum_{j=1}^{n} (r_1^j a_{2,j}^* - (r_2^j)^* a_{1,j}) \right] - x_1 \right|^2 + \left(-1 + \sum_{j=1}^{n} \sum_{i=1}^{2} \left| a_{i,j} \right|^2 \right) \left| x_1 \right|^2 \tag{4.9}$$

The above two equations are not complex and can be readily implemented. This is the benefit of space time block codes over the trellis-based space time codes since they provide maximum diversity gain with little complexity at the receiver.

C H A P T E R 5

TRANSMIT DIVERSITY TECHNIQUES FOR CDMA SYSTEMS

5.1 Introduction

The World Wide Web and increasing demand for wireless services (e.g., voice and data) are driving the demand for increased system capacity, data rates, and multimedia services. The International Mobile Telecommunications in 2000 (IMT-2000) standards development process, within the International Telecommunication Union (ITU), is driving the development of enhanced third-generation (3G) standards in order to address current and future wireless service needs. Particularly the Third Generation Partnership Project (3GPP) and Third Generation Partnership Project Two (3GPP2) are developing the wideband code-division multiple access (WCDMA) technologies and CDMA2000, respectively. Improvement of downlink capacity is one of the main challenges facing the effort toward 3G evolution. Many of the proposed services are expected to be downlink intensive, and moreover likely to be used in low-mobility environments under single-path conditions. Poor performance due to prolonged deep fading of the channel is one of the problems associated with this model. Transmit diversity (TD) is one of the key contributing technologies to addressing this problem in these proposed 3G CDMA systems.

Multiple antennas can improve the performance of a wireless communication system in a fading environment [20]. Although multiple antennas may be employed at either the base station, mobile station, or both, it is most cost effective and practical to employ multiple antennas at the base station. Hence, the topic matter of this thesis is restricted to the case of employing multiple antennas at the base station.

The spacing of the antennas also affects the degree of correlation between the channels from the antennas to the mobile. Large antenna spacing, on the order of several carrier wavelengths, leads to uncorrelated fading, which leads to maximum performance gain due to spatial diversity. Beamforming methods, on the other hand, utilize antenna spacing less than the carrier wavelength, typically half the wavelength.

5.2. Transmit Diversity Basics

5.2.1. Delay Diversity

Delay diversity for two antennas, shown in Figure 5.1a, is a simple TD scheme that helps combat flat fading. Bits in Figure 5.1 are generated by a source consisting of information from a computer, a digitized speech signal, or after being encoded by a channel encoder. The bits are numbered such that a bit at time instant n is denoted $b[n]$. The original bits are transmitted using two antennas, where the first antenna transmits without delay and the second sends $b[n]$ after a delay of one or more sample instants. The resulting waveform at the input to the receiver is

$$\begin{aligned} X_d(t) &= a_1(t)\sum_n b[n]c(t-nT) + a_2(t)\sum_n b[n-1]c(t-nT) + \gamma(t) \\ &= \sum_n b[n]a_1(t)c(t-nT) + a_2(t)c(t-(n+1)T) + \gamma(t) \end{aligned} \tag{5.1}$$

where a_k is the fading coefficient for an independent flat fading channels, $c(t)$ is the modulating waveform for each bit, and T is the amount of time each bit is transmitted before moving to the next bit. The effect of delay diversity on a slowly fading channel is to allow the receiver to coherently add the two independent fading channels together to aid in demodulation. Typically, unique pilot symbols are sent on each antenna, allowing the receiver to characterize the two channels formed between each antenna and the mobile. Considering a case where $a_1(t)$ and $a_2(t)$ are identically distributed complex Gaussian random processes, the response of of channel is given by $\alpha(t) = \left(|a_1(t)|^2 + |a_2(t)|^2\right)^{1/2}$. The fade depth, difference between the peaks and valleys, is less than that experienced in single path case. Thus, the resultant channel is more reliable from a communication perspective.

This approach suffers from reduced throughput due to multiple transmissions of the same symbol over time. Another instance of delay diversity may be achieved in multipath channels where the signal bandwidth is larger than the coherence bandwidth of the channel; in this case the multipaths are resolvable and may be recovered by a rake receiver. Frequency diversity methods similarly can improve the receiver performance in the presence of flat fading.

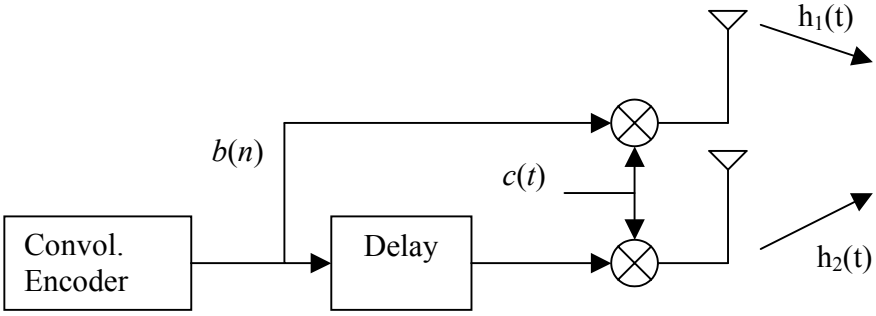

Figure 5.1 Delay diversity.

5.2.1. Frequency Diversity

Frequency diversity methods (Figure 5.2) employ transmission of multiple symbol replicas over multiple carriers, each separated in frequency by a sufficiently large amount to ensure independent fading. To ensure independent fading employing this technique, the difference between the two carriers, f_{c1} and f_{c2}, must be greater than the coherence bandwidth (i.e., $|f_{c1} - f_{c2}| \geq B_c$).

Using notation as described in the previous section, the resulting waveform at the input to the receiver is

$$\begin{aligned} X_{d(t)} &= a_1(t)\sum_n b[n]e^{j2\pi f_{c1}(t-nT)} + a_2(t)\sum_n b[n]e^{j2\pi f_{c2}(t-nT)} + \gamma(t) \\ &= \sum_n b[n]\left\{a_1(t)e^{j2\pi f_{c1}(t-nT)} + a_2(t)e^{j2\pi f_{c2}(t-nT)}\right\} + \gamma(t). \end{aligned} \tag{5.2}$$

Similar to TD, the effect of frequency diversity for a slowly fading channel is to allow the receiver to coherently add the two independent fading channels together to aid in demodulation. This approach is accompanied by the additional cost of increased complexity at both the transmitter and receiver, along with the fact that it may be difficult to implement in bandwidth-limited systems. Given this brief overview of TD basics, our attention focuses more specifically on the issues of TD in the context of 3G CDMA evolution. Several methods of TD have been proposed for 3G CDMA evolution. These can be broadly categorized into *open loop* and *closed loop* techniques.

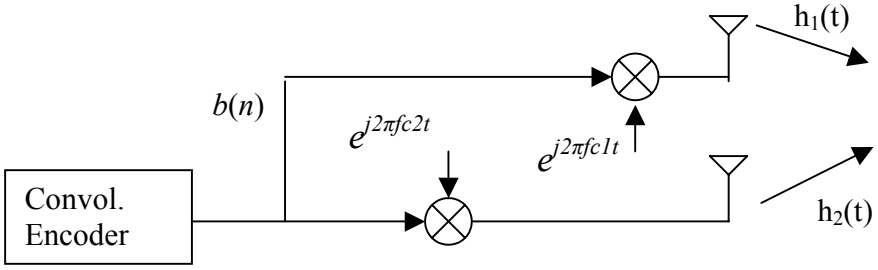

Figure 5.2 Frequency Diversity.

5.3 Open Loop Transmit Diversity in CDMA

In open loop diversity methods, a predetermined form of diversity is introduced using multiple antennas. Advantages of this class of methods include:

- Signaling overhead is not required to achieve this form of diversity.
- The mobile station (MS) receiver complexity is kept relatively low.

The most obvious disadvantage is that the channel environment information is not utilized; that is, open loop techniques are a *one-size fits all* approach to achieving TD for all mobile users.

The earliest open loop diversity techniques were simple in their configuration, for example, *phase-switched TD* (PSTD) and *time-switched TD* (TSTD). PSTD introduces a known periodically varying phase difference between the symbols transmitted through different antennas to simulate fast fading. In TSTD the transmission is switched among the different antennas with a known periodicity. All antennas transmit the same symbol simultaneously at reduced power, so the total power remains unchanged. Each of these methods has been proposed at one time or another in the 3G CDMA standards bodies. TSTD was adopted for use on the synchronization channel in 3GPP. However, PSTD was not adopted in favor of other techniques such as *orthogonal TD* (OTD) [21], *space-time TD* (STTD) [3], *space-time spreading* (STS) [21], and *space-time coding-assisted double spread rake receiver* (STC-DS-RR) [22].

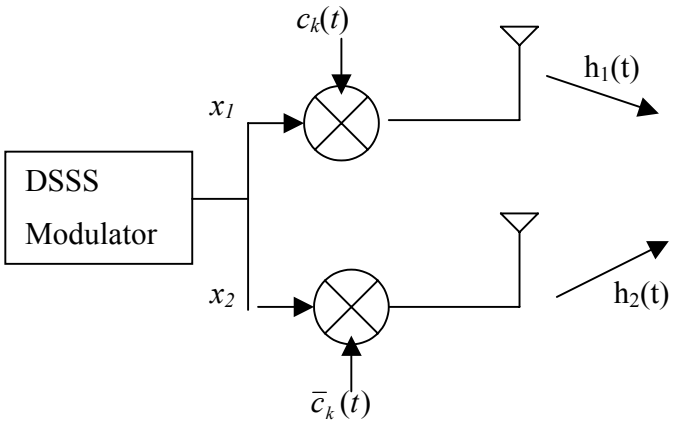

Figure 5.3. OTD transmitter.

5.3.1 Orthogonal Transmit Diversity

Orthogonal TD [21] is an open loop method in which coded interleaved symbols are split into even and odd symbol streams and transmitted using two different Walsh codes. The length of the Walsh code is doubled so that the total number of Walsh codes available is not reduced as a result of splitting the data, and the data rate will remain more constant than is the case with no data splitting. Consider the two-antenna case. Let x_1 and x_2 be the even and odd symbols, respectively. Then the symbols transmitted over the two antennas, s_1 and s_2, are given by

$$\begin{aligned} s_1 &= x_1 c, \\ s_2 &= x_2 c^*, \end{aligned} \tag{5.3}$$

where c, $c*$ are complementary Walsh codes used (same chip rate, covering twice as many chips as in the absence of OTD, but in the same number). The signal received at the mobile receiver will be

$$r = h_1 s_1 + h_2 s_2 + \gamma \tag{5.4}$$

where h_1, h_2 are the channels from the two antennas to the MS, as shown in Figure 5.3. The time subscripts have been left out for brevity. The received signal from the two antennas is despread using the same Walsh codes, and then combined to recover the original symbol stream.

5.3.2 Transmit Diversity Via Space-Time Coding

Space-time coding is a means of enhancing the level of diversity presented to a receiver in a wireless link, via the addition of TD and in order to more efficiently combat the signal fading inherent to wireless communication channels. Motivated by the information theoretic results by Foschini and Gans [23] and Telatar [24], early ideas on TD schemes (e.g., delay diversity, in which a second antenna transmits a delayed replica of another transmit antenna's signal) have been refined by the work of Tarokh *et al.* [25]. Since it is advantageous to separate the problem of combating fades from that of channel equalization, the criteria for designing space-time codes are usually derived in the context of narrowband modulation and frequency nonselective fading. The noteworthy fact about this approach is that it isolates TD from those forms of diversity associated with the radio channel (e.g., due to multipath). Nevertheless, spread spectrum systems in frequency selective channels can benefit equally from coding with space and time redundancy, as outlined below.

In general, coding with space and time redundancy is accomplished by finding an efficient way to allocate different symbols to different antennas while adding, jointly across antennas, some type of time redundancy for implementing forward error correction. For each of the symbol streams associated with different antennas, the system can then resort to other means to combat frequency selective fading. For example, orthogonal frequency-division multiplexing (OFDM) naturally lends itself to being used in conjunction with TD; likewise, when the excess delay is small, space-time block coding (see below) can easily be used in a maximal ratio-combining receiver for frequency selective channels.

Space-time coding can be implemented in either block [3], [25], or trellis form [26] as discussed in the previous chapter.

In the case of full rate transmission, $k = p$, where k is the number of symbols that will have to be decoded and p is the number of time slots it takes to transmit all the symbols. In this situation, an orthogonality property for the square space-time block code matrices [25], allows easy recovery of the symbols arriving from different transmit antennas despite their superposition (in time) at the receiver's input. For complex modulator constellations the only known rate one constructions are 2×2 (i.e., for two

transmit antennas). The construction for two transmit antennas was first proposed by Alamouti in [3] and is defined by the simple 2×2 pattern,

$$\begin{bmatrix} x_2 & x_1 \\ -x_1^* & x_2^* \end{bmatrix}, \tag{5.6}$$

where x_1 , x_2 are valid complex symbols from the signal constellation (same on both antennas). Matrices like this are unitary, cover two symbol epochs, and allow easy recovery of x_1 , x_2 at the receiver given the channel state [3], [25]. Alamouti's idea, based on the Hurwitz-Radon transform, was further refined by Tarokh *et al.* [25].

5.3.2.1 Space-Time Transmit Diversity

STTD is an open loop technique in which the symbols are modulated using the technique described in [3]. This type of open loop TD has been adopted by the 3GPP because this type of transformation maximizes diversity gain.

STTD is defined for two antennas. Assume once again that x_1 and x_2 are the even and odd symbols, respectively. Then the transmissions over the two antennas, s_1 and s_2 are given by

$$\begin{aligned} s_{11} &= x_2 c, \\ s_{21} &= x_1 c, \\ s_{12} &= -x_1^* c, \\ s_{22} &= x_2^* c, \end{aligned} \tag{5.7}$$

where c is the orthogonal Walsh code.

The received symbol is decoded over two consecutive time epochs. The received symbol may be represented in vector form as

$$\begin{bmatrix} r_1 \\ r_2 \end{bmatrix} = \begin{bmatrix} h_1 x_2 c + h_2 x_1 c \\ -h_1 x_1^* c - h_2 x_2^* c \end{bmatrix} + \begin{bmatrix} n_1 \\ n_2 \end{bmatrix}. \tag{5.8}$$

Neglecting the Walsh codes, an estimate of the transmitted symbols may be formed as

$$\begin{bmatrix} \hat{x}_1 \\ \hat{x}_2 \end{bmatrix} = \begin{bmatrix} h_2^* r_1 - h_1 r_2^* \\ h_1^* r_1 + h_2 r_2^* \end{bmatrix}. \tag{5.9}$$

The STTD scheme is particularly simple, in the sense that it implements Alamouti's space-time block code (2×2 code matrices, see above) and follows it by separate spreading and scrambling, as in the non-diversity mode. The orthogonality property of the code matrices allows the symbols from the two transmit antennas to be separated at the receiver front-end. There is no need for separate Walsh codes on the two transmit antennas for the traffic channel because the orthogonality between space-time code matrices is realized in the time domain, just as in frequency nonselective fading. However, separate Walsh codes are needed for the antenna pilot signals in order to distinguish the channels.

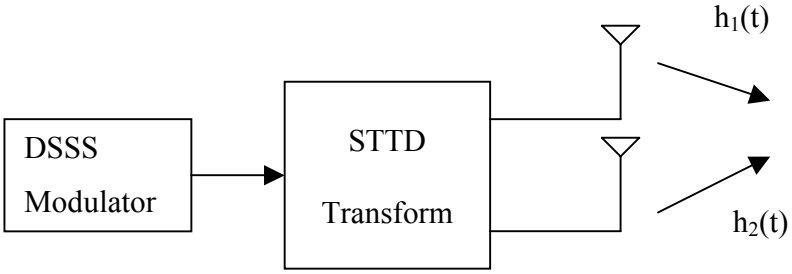

Figure 5.4 STTD transmitter.

5.3.2.2 Space-Time Spreading

STS [21] is another open-loop technique in which the symbols are spread using multiple Walsh codes. It differs slightly from STTD, as explained below. Of course, apart from Walsh spreading, the symbols are spread by a long spreading code, but this will be self-understood and omitted here for simplicity. The differences from STTD arise in the need for STS to be compatible with certain details of the IS-2000 specifications, in particular OTD. This was not the case within the 3GPP standard, which made the implementation of STTD much more straightforward.

We have a generic transmit diversity system that employs M transmitter and N receiver antennas. We will denote this as an (M, N) system. In transmit diversity, the information-bearing input signal $x(t)$ is demultiplexed in $s_m(t)$, m = 1,... ,M, each of which is transmitted (after up-conversion) by the mth antenna. In DS-CDMA, each symbol of the information-bearing sequence $\{x(i)\}$ of a particular user is spread by a code sequence $\mathbf{c}_i=[c_i(1)\ldots..c_i(N)]^T$ where N is the spreading factor and T denotes vector transpose. This

spreading operation can be represented mathematically simply as $s(i) = x(i)c_i$, where $s(i)$ is the N x 1 vector that contains a block of N consecutive (chip-rate) samples corresponding to the user's i-th symbol period. In the forward link, c_i typically repeats itself in each symbol period ($c_i = c$), however, for the purpose of presenting transmit diversity schemes, we will not impose this restriction. When multiple antennas are available at the transmitter, emergs as choosing the way that the user's information sequence $\{x(i)\}$ is spread on each antenna a new task. One naive choice would be to spread the user's signal in the same exactly fashion on each antenna, i.e. $s_m(i) = c_i x(i)$. However, such a scheme would offer no diversity gain at the receiver, since the system would be equivalent to transmitting from a single antenna with the same total transmitted power. An interesting alternative would be to use a different code to spread the user's signal on each different antenna, i.e. $s_m(i) = \mathbf{c}_i^m x(i)$, where $\left\{c_i^m,\ m = 1,...,M\right\}$ is a set of orthogonal codes $\left(\mathbf{c}_i^{mT}\mathbf{c}_i^n = \delta_{mn}\right)$ where δ is the Kronecker delta. Such a scheme provides an important diversity advantage at the receiver, however it requires M times more orthogonal codes.

Consider now that each user's data is split into K sub-streams $\{x_1\},\ldots,\{x_k\}$, Such that $x_k(i) = x\left(\left(i-k\right)K + k\right),\ \ k = 1,...,K$. Then we will allow each sub-stream $x_k(i)$ to be spread by a different code c_k (same for all symbols in that sub-stream). Space-time spreading STS), as introduced in [27], [28], relies on the following observation: each user's transmitted signal from each antenna $s_m(i)$ can in general be a different combination of the user's sub-streams and corresponding spreading codes, without necessarily using more than 1 code / sub-stream, i.e.

$$s_m(i) = \mathbf{f}_m\left(x_1(i),...,x_K(i),\mathbf{c}_1,...,\mathbf{c}_K\right) \tag{5.10}$$

The design of functions $\left\{\mathbf{f}_m(\cdot)\right\}$ that allow for a "clever" re-use of code signatures across the different antennas so as to provide maximal diversity gain at the receiver with relatively simple processing then becomes an interesting problem.

In the STS scheme first introduced publicly in [27], the transmitted signals from the two antennas are shown in Figure 5.5

$$\begin{aligned}\mathbf{s}_1(i) &= 1/\sqrt{2}\left(x_1(i)\mathbf{c}_1 + x_2(i)\mathbf{c}_2\right)\\ \mathbf{s}_2(i) &= 1/\sqrt{2}\left(x_2(i)\mathbf{c}_1 + x_1(i)\mathbf{c}_2\right)\end{aligned} \tag{5.11}$$

where $\{x_1(i)\}$, $\{x_2(i)\}$ represent the odd and even user information-bearing sequences and the normalization by $\sqrt{2}$ is used to normalize the total transmit average power to unity. Assuming single-path propagation, the channel from the *m*th antenna to the single receive antenna is represented by the complex scalar h_m . The received signal can be written as $r(i) = 1/\sqrt{2}\left(h_1\left(x_1(i)\mathbf{c}_1 + x_2(i)\mathbf{c}_2\right) + h_2\left(x_2(i)\mathbf{c}_2 - x_1(i)\mathbf{c}_2\right)\right) + \gamma(i)$ where $\boldsymbol{\gamma}^T(i) = \left[\gamma_1(i)\ \ \gamma_1(i)\right]$ is the additive noise vector. The receiver despreads the received signal separately with $\mathbf{c}_1$ and $\mathbf{c}_2$ to yield:

$$\begin{aligned} d_1(i) &= \mathbf{c}_1^T\mathbf{r}(i) = (1/\sqrt{2})(h_1x_1(i) + h_2x_2(i) + \gamma_1(i) \\ d_2(i) &= \mathbf{c}_2^T\mathbf{r}(i) = (1/\sqrt{2})(-h_2x_1(i) + h_1x_2(i) + \gamma_2(i) \end{aligned} \tag{5.12}$$

where $\gamma_m(i) = \mathbf{c}_m^T\gamma(i),\ m = 1,2$. Equation (3) can be equivalently written as

$$\begin{aligned} \mathbf{d}(i) &= \left(1/\sqrt{2}\right)\begin{bmatrix} h_1 & h_2 \\ -h_2 & h_1 \end{bmatrix}\begin{bmatrix} x_1(i) \\ x_2(i) \end{bmatrix} + \gamma(i) \\ &= \left(1/\sqrt{2}\right)\mathbf{H}\mathbf{x} + \gamma(i) \end{aligned} \tag{5.13}$$

where $\boldsymbol{\gamma}^T(i) = \left[\gamma_1(i)\gamma_2(i)\right]$. Notice that **H** is a unitary matrix. Simple matched-filter processing then yields

$$\mathrm{Re}\left\{\mathbf{H}^H\mathbf{d}(i)\right\} = \left(1/\sqrt{2}\right)\left(\left|h_1\right|^2 + \left|h_2\right|^2\right)\mathbf{x}(i) + \boldsymbol{\gamma}'(i) \tag{5.14}$$

hence two-branch diversity combining is achieved at the receiver. Notice that this is being done by using no extra resources (such excessive codes or transmit power) and no feedback from the subscriber unit.

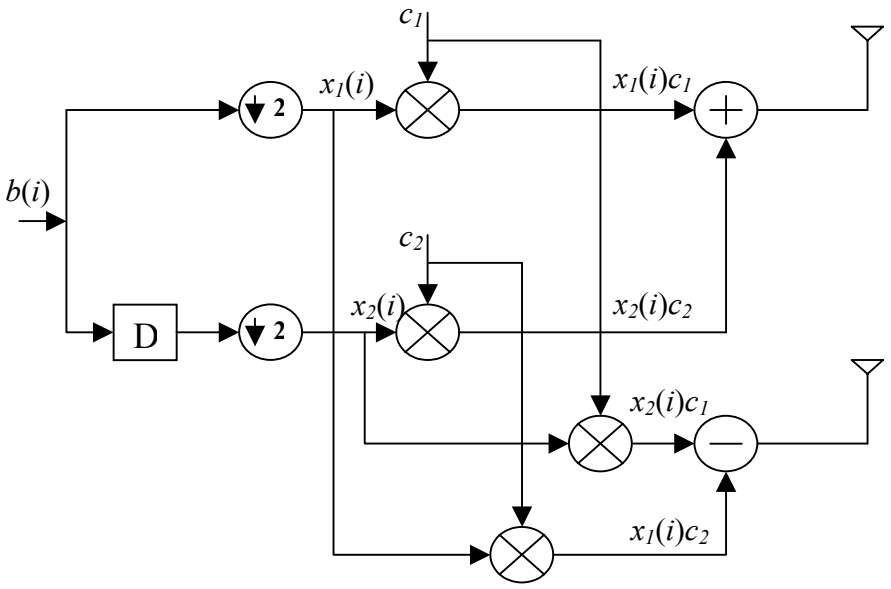

Figure 5.5 STS transmit diversity scheme

5.3.3 Space-Time Coding-Assisted Double Spread System

This open loop technique was proposed by L. Hanzo for downlink transmissions over fading channels [22]. It is slightly differs from STTD systems. There are two spreading stages. Specifically, in the first spreading operation unique user signature Walsh codes are used for distinguishing the users and hence mitigating the effects of MAI, while in the second spreading step a random code is employed for spreading and hence attaining path diversity.

The block diagram of the Space-Time Coding-Assisted Double-Spread Rake Receiver (STC-DS-RR) based CDMA scheme proposed for downlink transmission is shown in Figure 5.6. S_i is spread by the Walsh code c_i^W, where each user is assigned a unique Walsh code. The sum s of the signals of all users is then passed to the STBC encoder on a chip by chip basis. Here Alamouti's G_2 code associated with two transmit antennas is used for STBC. The STBC encoder yields two chips, namely d_1 and d_2, one for each transmit antenna. Both chips are then spread by the same random code, namely c^R

before transmission through the L-path dispersive Rayleigh fading channels associated with the two transmission antennas. A single Rake receiver is utilized at the mobile station. The Rake receiver then produces L outputs, $y_1, \ldots y_L$, each to be despread by the random code c^R, where each of the L despread signals benefits from transmit diversity of order two due to the STBC. Consequently, the STBC decoder is invoked L times, namely once for each of the L despread outputs for obtaining path diversity of order L. The L STBC decoded signals are summed, yielding $\hat{s}$, which has a total diversity order of $2L$. Then, the signal $\hat{s}_i$ of user-k can be obtained by despreading $\hat{s}$ with the aid of the unique Walsh signature sequence c_i^W .

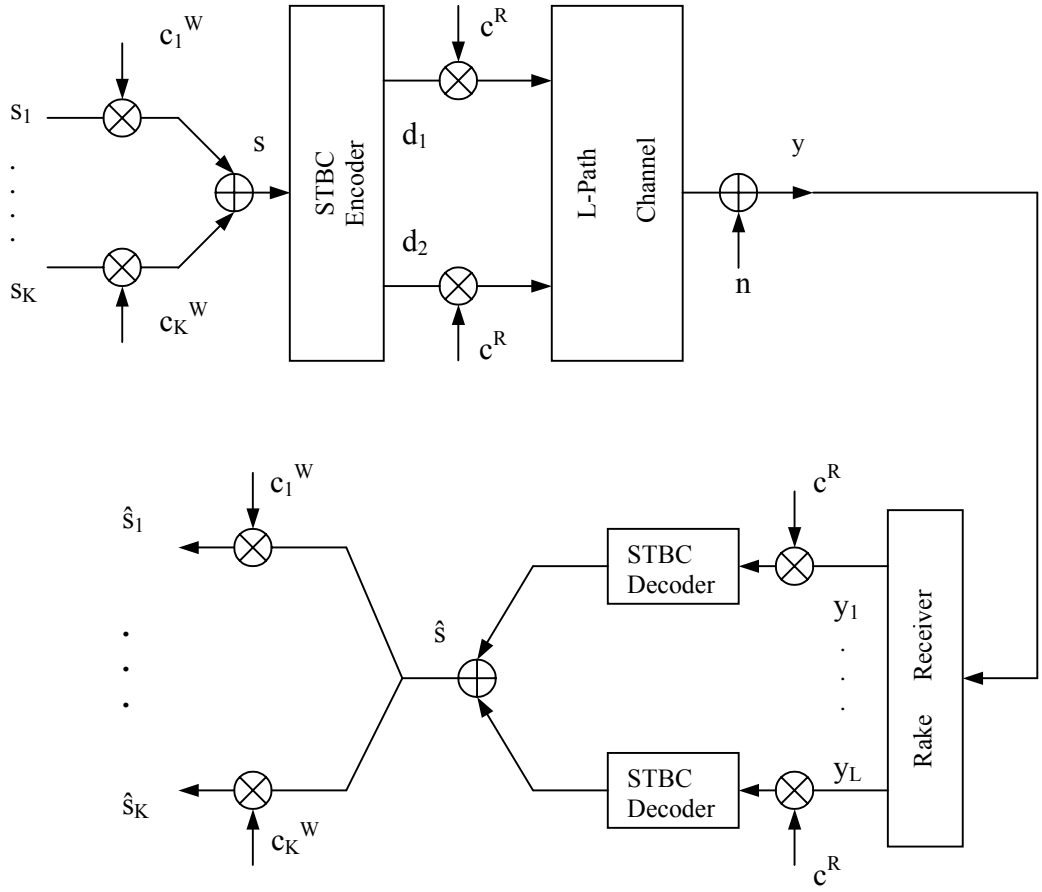

Figure 5.6 The block diagram of the Space-Time Coding-Assisted Double-Spread Rake Receiver (STC-DS-RR) based CDMA scheme.

5.3.3.1 Double-Spreading Mechanism

Walsh codes are well known for their attractive zero cross correlation property,

$$\sum_{l=1}^{N} c_i^W[m].c_j^W[l]=0 \ ; \ \text{for } i \neq j, \tag{5.15}$$

there are N chips in a code and the maximum number of Walsh codes of length N is N, which can support a maximum number of $K=N$ users. Therefore it is possible to support N users employing Walsh codes of length N without encountering MAI, provided that the codes' orthogonality is not destroyed by the channel. However, the auto-correlation of Walsh codes is relatively high.

$$\sum_{l=1}^{N} c_i^W[m].c_i^W[l]\neq 0 \ ; \ \text{for } m, \ i \in \{1...N\} \tag{5.16}$$

Hence, the good cross-correlation properties of Walsh codes are easily destroyed by the multi-path interference encountered in dispersive channels. In contrast to Walsh codes, random codes exhibit high cross-correlation but low auto-correlation values. Therefore random codes can be beneficially processed by a rake receiver for obtaining path diversity due to their low auto-correlation value. However, without additional Walsh spreading they are only applicable for single user scenarios, since the associated high cross-correlation will result in intolerable MAI.

The double-spreading mechanism invokes $\bar{N}$-chip Walsh codes for supporting K= $\bar{N}$ users and additionally a $\tilde{N}$-chip random code for attaining multi-path diversity, where there are N chips per information symbol and we have $\bar{N} \times \tilde{N}$ = N. The first spreading operation spreads each information symbol of user-i to $\bar{N}$ chips, using the Walsh code c_i^W. Then the $\tilde{N}$-chip random code further spreads each of the resultant chips to $\bar{N}$ chips. Hence there are a total of $\bar{N}$ x $\tilde{N}$ = N chips per information symbol according to the conventional method highlighted above, although the spreading mechanism used is different. Here, the same $\tilde{N}$-chip random code repeats itself every $\tilde{N}$ chips, namely for each of the Walsh-code chips. Note that the lth chip of the $\tilde{N}$-chip Walsh code of all users is spread by the same random code, which are conveyed via the same channel and experience an identical multi-path interference of:

$$I[l] = I_k[l] = I_i[l] \tag{5.17}$$

where k, i $\in$ {1 . . . $\bar{N}$ } and $I[l]$ is the interference imposed on the lth chip of user-k's Wash code, $c_k^{\,W}[l]$. If a slow fading channel is encountered, the Channel Impulse Response (CIR) of the multi-path components of the channel can be assumed to be time-invariant for the duration of N.

$$I = I[l] = I[m];\ l, m \in \left\{1 \ldots \bar{N}\right\}. \tag{5.18}$$

resultant cross correlation of the codes can be shown to be zero, which is expressed as:

$$\begin{aligned} \sum_{l=1}^{\bar{N}} \left(c_i^{\,W}[l].I_i[l]\right).\left(c_k^{\,W}[l].I_k[l]\right) &= I^2.\sum_{l=1}^{\bar{N}} c_i^{\,W}[l].c_k^{\,W}[l], \\ &= 0 \ ; \text{for } i \neq k. \end{aligned} \tag{5.19}$$

This implies encountering no MAI, hence requiring no MUD. Therefore attaining near-single-user performance is feasible with the advent of this simple double-spreading method without the employment of complex MUD schemes in slow fading dispersive channels.

5.3.3 Schemes For More Than Two Antennas

Theoretically, the number of antenna elements through which independent channels can be transmitted bound the achievable order of spatial diversity. A few open loop schemes have been proposed for four antennas:

• A concatenation of the OTD scheme mentioned earlier and the STS scheme has been proposed as a diversity technique using four antennas [29].

• An extension of the Alamouti scheme in an earlier section for three or four antennas called *ABBA* has been proposed [30]. It has been proven that orthogonal designs do not exist for complex channels for four antennas. Hence, this is a suboptimal construction, which involves some interference cancellation along with space-time decoding.

5.4 Closed Loop Transmit Diversity In 3G

Closed loop diversity techniques are adaptive in nature. The BS obtains knowledge of the downlink channel from the MS via feedback signaling, and uses this knowledge to its advantage. The use of feedback in transmit antenna arrays was first proposed by Gerlach and Paulraj [31] as *transmit beamforming*. They proposed that training signals be transmitted periodically on the downlink and the responses of the various MSs fed back to the BS. This information is used to calculate the optimal transmit weights for each mobile such that the received power at the desired MS is maximized and interference to other MSs is minimized. These TD techniques can be described as customized to fit the channel conditions for each mobile user. As explained at the beginning, the goal of inducing diversity runs somewhat contrary to that of inducing directionality using beamforming in that the antennas have to be spaced far apart. But the problem formulation for calculating the antenna weights remains the same if one recognizes the fact that knowledge of the different channel coefficients is equivalent to knowledge of the directional array manifold vector in the case of beamforming. In this sense, the closed loop diversity techniques considered in the 3G standards are variants of the approach in [31]. In fact, correlated fading models for multiple antennas and closed loop solutions have been considered recently in these forums. When operators are constrained by considerations of space from placing antennas which are close to each other at the BS.

C H A P T E R 6

EXPERIMENTAL RESULTS

6.1. Introduction

In this chapter, the computer models for a CDMA-based space-time coded forward channel system are presented and simulation results analyzed. While the simulations are designed, all transmit diversity schemes are considered separately. In order to get good comparisons with each simulation; same channel coefficients, spreading factors and number of users are used. The simulation uses both the two-ray Rayleigh fading [7] and flat fading Rayleigh channel models. Firstly, for the flat Rayleigh fading channel model, the performances of OTD, STTD and STS are compared. Then, for the two-ray Rayleigh fading channel model, the performances of no transmit diversity system and space-time coding-assisted double spread system are investigated.

6.2. Multipath Model

Multipath propagation is used to add some realism to the performance of a channel in a true wireless environment. For a wideband signal, the channel bandwidth is considerably smaller than the signal bandwidth leading to frequency selective fading. The received signal will consist of multiple copies of the original signal attenuated and delayed in time. This leads to ISI in the time domain. While frequency selective fading describes the brief snapshot of the channel a user's signal encounters, it is necessary to define the rate of change of the channel impulse response in time. A slow fading channel occurs when the rate of change of the channel characteristics is much slower than the symbol duration of the signal. Fast fading occurs when the channel changes faster than a symbol. To minimize computation, only slow fading was considered in this simulation; the channel impulse response was maintained constant over a frame duration. The baseband impulse response of a channel may be mathematically represented as [32]:

$$h(t,f) = \sum_n a_n \exp(-j\omega\tau_n)\exp(-j2\pi f_D t) \tag{6.1}$$

where a_n and τ_n are complex gain and time delay of the *n*th multipath component and f_D is the Doppler shift. Assuming wide sense stationary over a small-scale time interval the channel impulse response may be simplified to

$$h(t) = \sum_{n=0}^{N-1} a_n \exp(-j\theta_n)\delta(t-\tau)\,. \tag{6.2}$$

The weights a_n are assumed to be Gaussian and θ_n are uniformly distributed in the interval [0,2π]. To compare multipath channels, mean excess delay and rms delay spread are often used. The mean excess delay is defined as

$$\bar{\tau} = \frac{\sum_n a_n{}^2 \tau_n}{\sum_n a_k{}^2} \tag{6.3}$$

and the rms delay spread is given by

$$\tau_{rms} = \sqrt{\frac{\sum_n a_n{}^2 \tau_n}{\sum_n a_k{}^2} - \left(\bar{\tau}\right)^2}\,. \tag{6.4}$$

A commonly used multipath model [7] is an independent Rayleigh fading two-ray model. Figure 6.1 shows a block diagram of the two-ray independent Rayleigh fading channel model. The impulse response of the model is represented as

$$h_b(t) = \alpha_1 \exp(j\phi_1)\delta(t) + \alpha_2 \exp(j\phi_2)\delta(t-\tau)\ . \tag{6.5}$$

Our other assumptions about the channel parameters, transmit power and number of data which is used in the simulations are following:

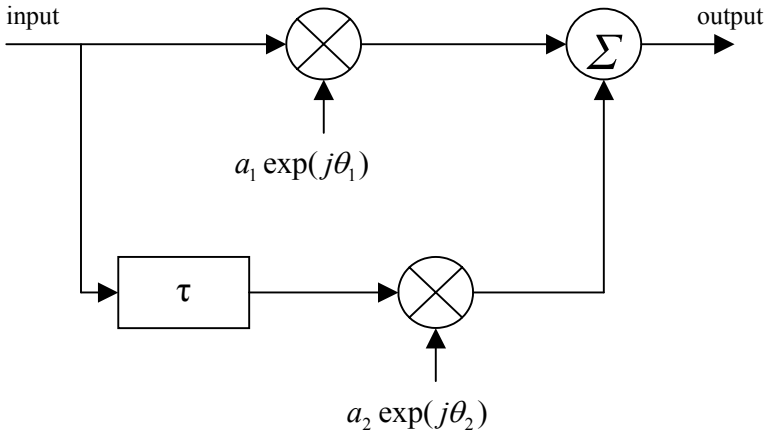

Figure 6.1 Two-ray Rayleigh fading model.

- The receiver interference and noise are assumed to have Gaussian distribution with zero mean and variance $\sigma^2 = 0.5/\text{SNR}$ per complex dimension.
- Channel from each transmitter antenna to the receiver antenna comprises 2 distinct paths. The average energy for the first path is 0.7 and the average energy for the second path is 0.3.
- Each pair of paths from the two transmitter antennas arrives with the same set of delays to the receiver antenna.
- Path delays are approximately a few chips in duration and small compared to the symbol period so that intersymbol interference (ISI) can be neglected.
- Spreading codes are orthogonal and perfectly known at the receiver.
- We use independent complex Gaussian random variables with variance 0.5 per real dimension to model the path gains.
- Speed of remote unit, v, is assumed to be 6 km/hour.
- Operating carrier frequency, f_c , is assumed to be 1900 MHz.
- The fade coefficients are assumed constant over a block of transmitted code frame. This is a reasonable assumption given that the bit interval T_b is small when compared to the speed of change in a wireless channel described by the maximum Doppler frequency f_m. Choosing f_m = 10 Hz, this assumption is

almost obtained excluding the case where the same coefficients are used in one block.

- We transmit $4 \cdot 10^6$ bits in order to reach 10^{-5} of sensitivity level for bit error rate.
- Codes are real, unit norm and the input data is BPSK.
- Spreading gain is equal to 16 for all kinds of communication schemes in order to make meaningful comparisons between them.

6.3 CDMA System without Transmit Diversity

The designed CDMA communication system is suited to compare the performances of the communication link in the absence and the presence of transmit diversity. After mapping the bits 0,1 to the bits –1,1 in data mapper, respectively, then resulting signal is spreaded by c_k . Wideband signal is sent by transmit antenna to receiver antenna through the channel. For this simulation we use a two-ray Rayleigh flat fading channel model. All details of the channel is given in previous sections. In the presence of multipath, the same transmission scheme can be used, but a Rake type architecture is required at the receiver. We performed simulation with a Rake type architecture.

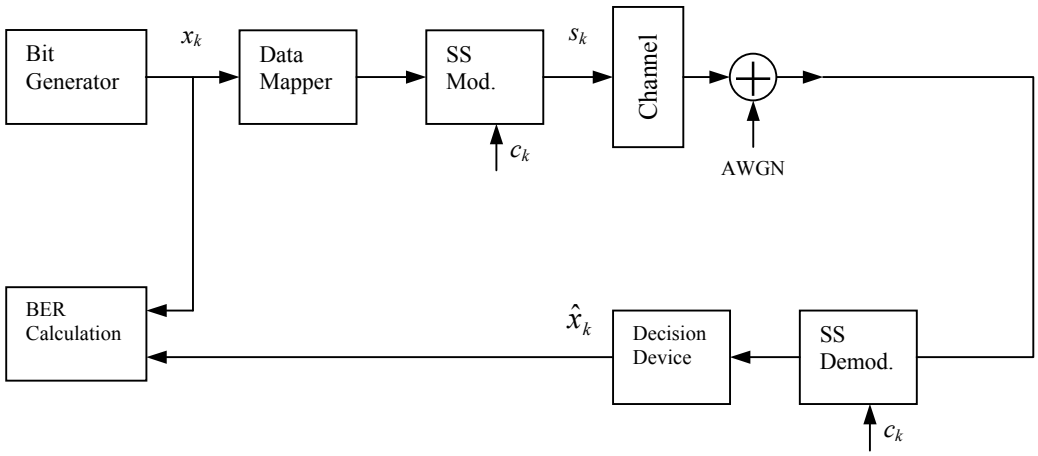

Figure 6.2 CDMA system without transmit diversity scheme.

Subsequent simulations are performed for two users because of two main reasons. Firstly, the code sequences are perfectly orthogonal to each other, thus the cross-correlations of these codes are equal to zero. According to our assumption, we know these codes at the receiver side, so we can recover the desired user's information bits without any MAI. Secondly, we assume for our two-ray Rayleigh channel model that the CSI and the corresponding time delay are known at the receiver side. Therefore the ISI is negligible and increasing the number of users in the communication system will not affect the performance of the communication link (Figure 6.3).

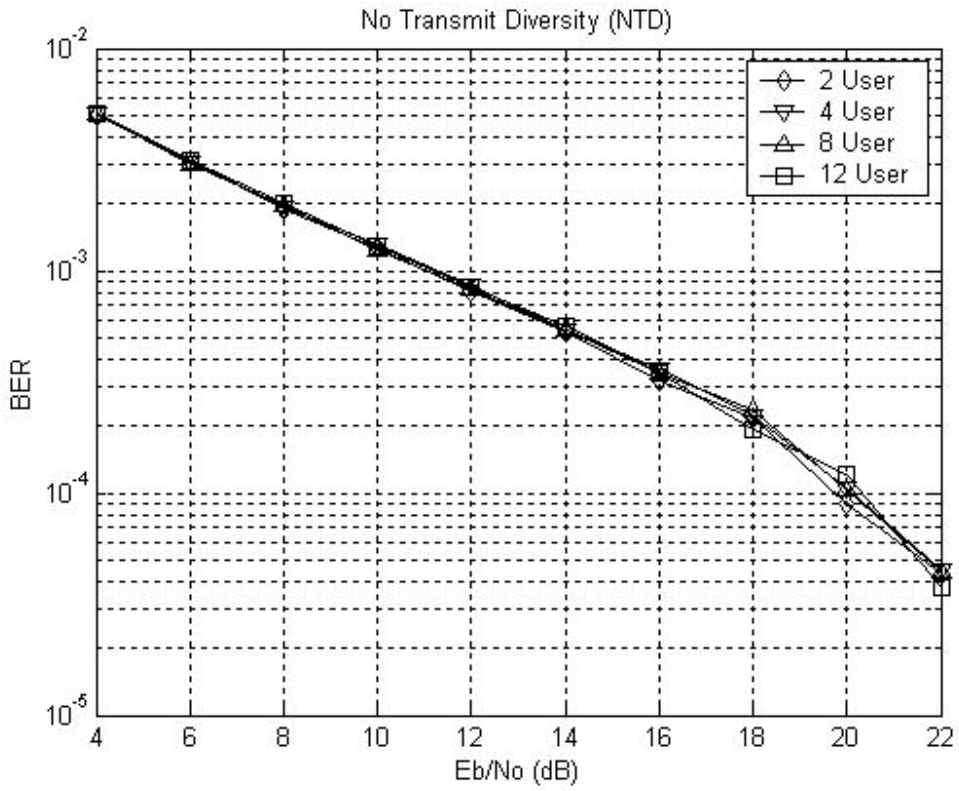

Figure 6.3 Performance of no transmit diversity case for different number of users.

6.4 Orthogonal Transmit Diversity

Orthogonal transmit diversity is implemented in the transmitter and the receiver as shown in Figure 6.4. The mapping bits are split into two different streams even and odd for simultaneous transmission over different antennas. Spread spectrum modulation is applied

to these two streams. The first antenna transmits the spread odd symbol periods and nothing during even symbols. Conversely, the second antenna transmits nothing during odd symbol periods and the spread even substream during even symbol periods. In this simulation the channel is assumed to be flat fading. So there is no need to use a Rake type receiver. The performance of OTD is highly dependent over one channel coefficients, as described how. At the receiver side, after despreading, recovered substreams are obtained as

$$\begin{aligned} \hat{x}_1 &= |h_1|^2 x_1 + h_1^* n \ , \\ \hat{x}_2 &= |h_2|^2 x_2 + h_2^* n \ . \end{aligned} \tag{6.6}$$

In a long fade of h_1 half of the user's data will be lost. The receiver recovers both even and odd data with the same diversity advantage, provided that not both h_1 and h_2 are simultaneously in a deep fade. This is the disadvantage of the OTD system over other techniques.

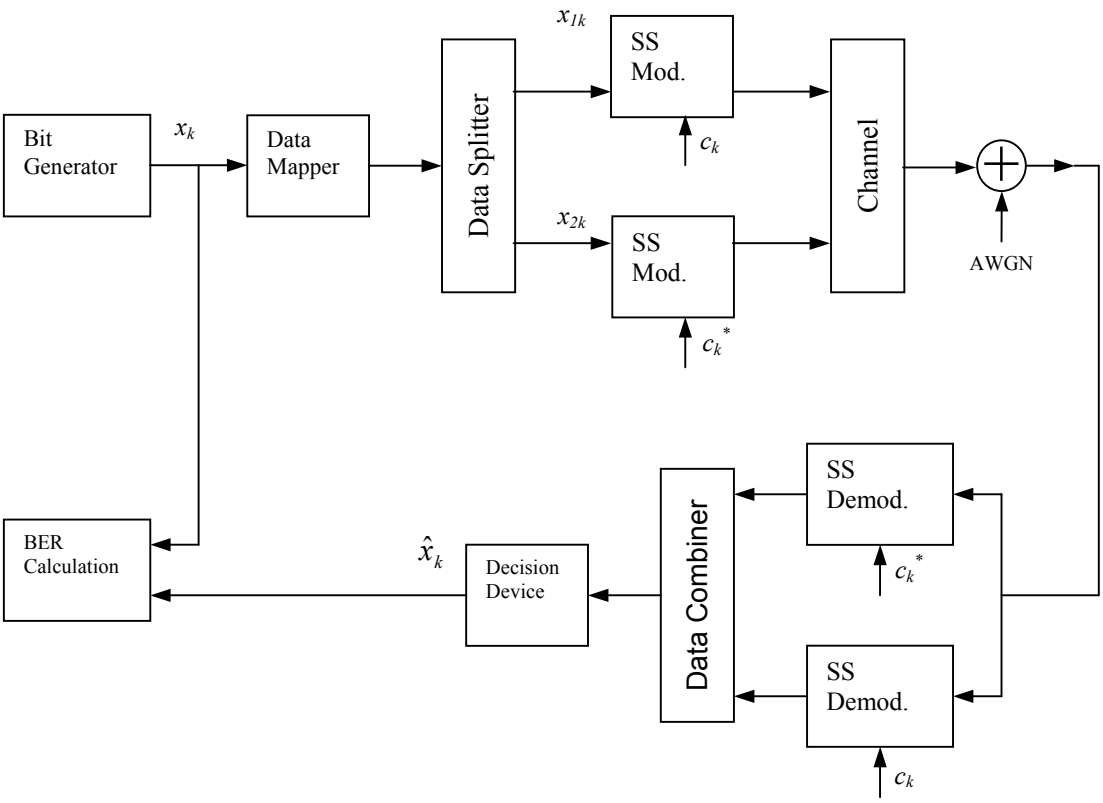

Figure 6.4 Orthogonal transmit diversity scheme.

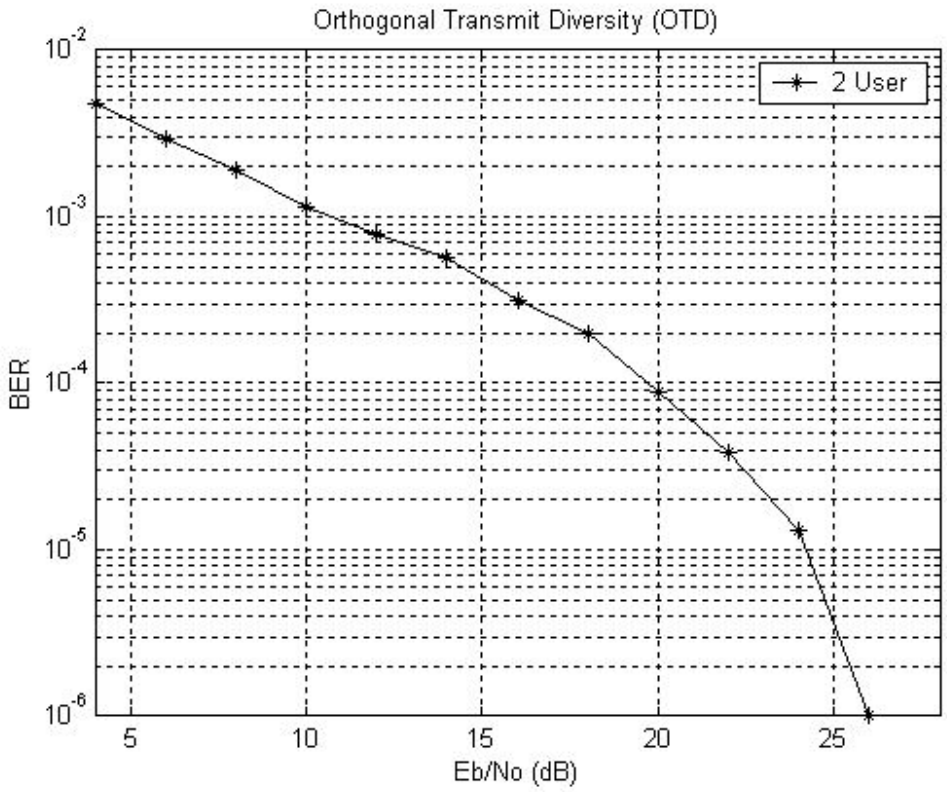

Figure 6.5 Performance of OTD case for 2 users.

6.5 Space-Time Transmit Diversity

Space-time transmit diversity is implemented in the transmitter and the receiver as shown in Figure 6.6. After spreading operation, spread signal is fed into STTD encoder. Output of the STTD encoder is sent to receiver antenna over a flat fading channel. At the receiver side STTD decoder and despreading operation are performed.

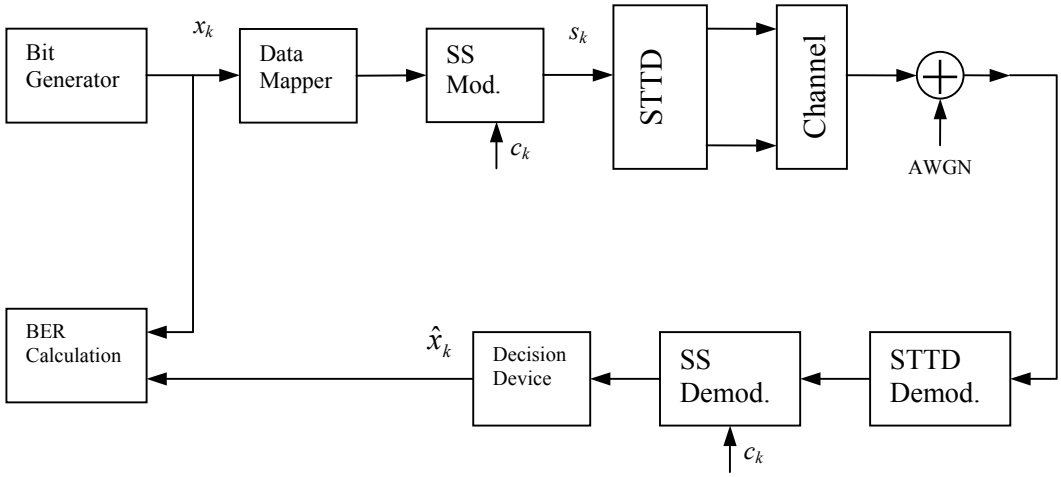

Figure 6.6 Space-time transmit diversity scheme.

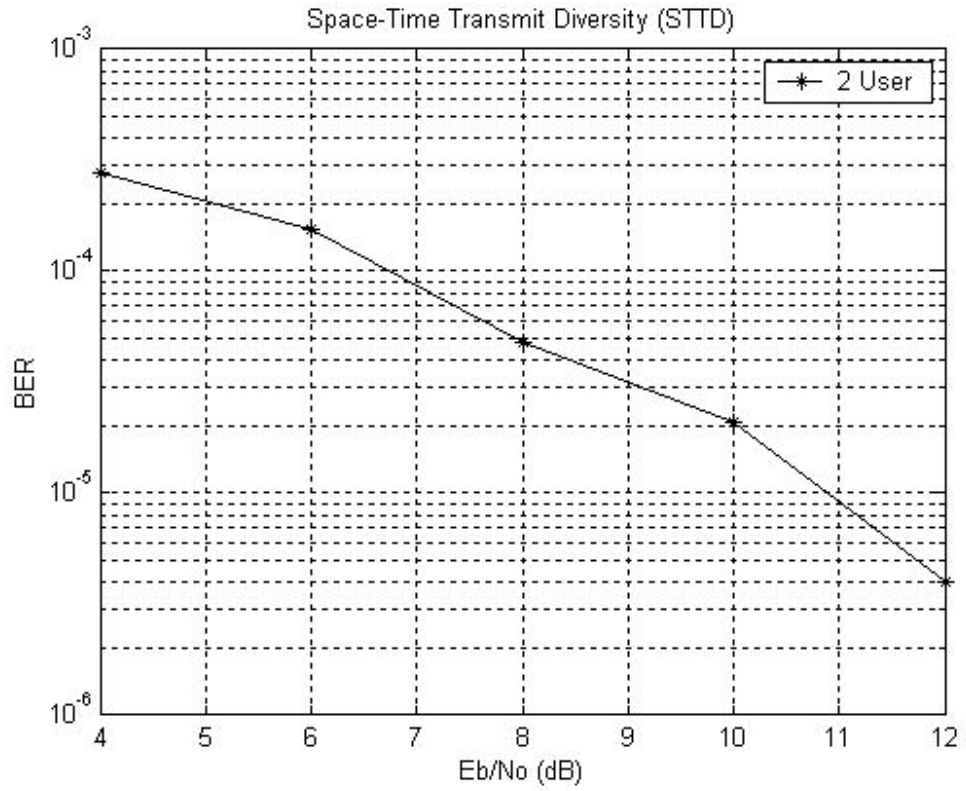

Figure 6.7 Performance of STTD case for 2 users.

6.6 Space-Time Spreading

Simulation scheme of STS is depicted in Figure 6.8. As in the OTD system, each user's data split into even and odd substreams, then spreading operation is performed as shown below. Spreading sequences are orthogonal. Similarly, in OTD, two spreading codes are used. The channel is assumed to be flat fading as in OTD and STTD.

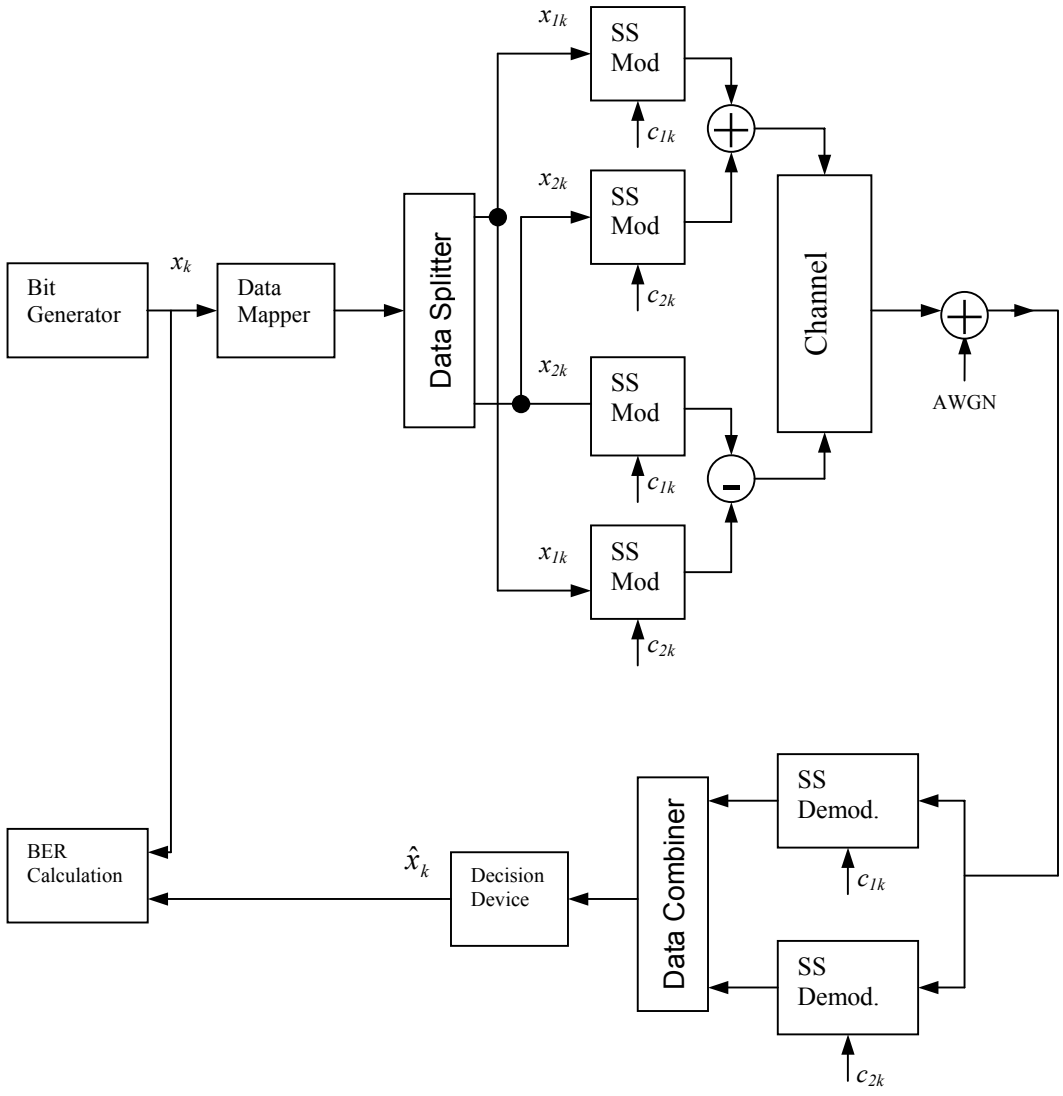

Figure 6.8 Space-time spreading scheme.

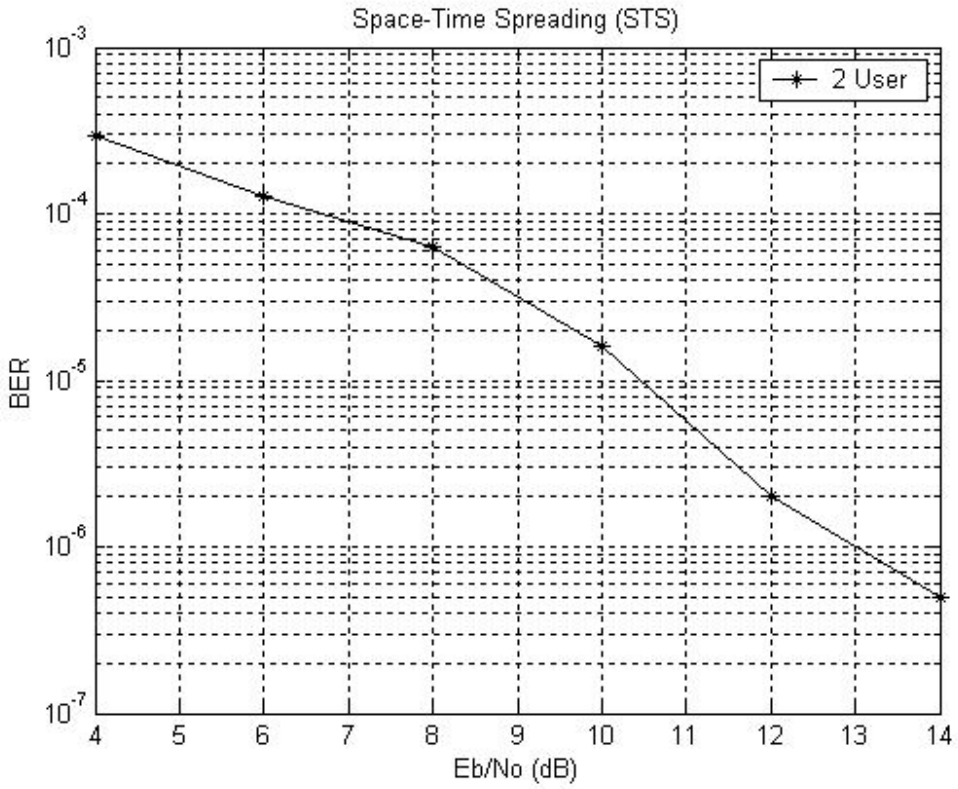

Figure 6.9 Performance of STS case for 2 users

6.7 Space-Time Coding-Assisted Double Spread System

Two stage spreading mechanism is combined with STBC encoding function. The simulated system and its performance is depicted in Figure 6.10 and 6.11, respectively. The processing gain of both the first and the second stages of the system are 4. Thus the total gain of the system is 16, which is equal to other simulation schemes. This gives us meaningful comparison chance. The channel model of the system is two-ray Rayleigh. Because of the presence of the multipath, at the receiver side, Rake receiver is used. The output of each Rake branch is connected to despreading and STBC decoder. Using Rake receivers adds additional receiver diversity to the system.

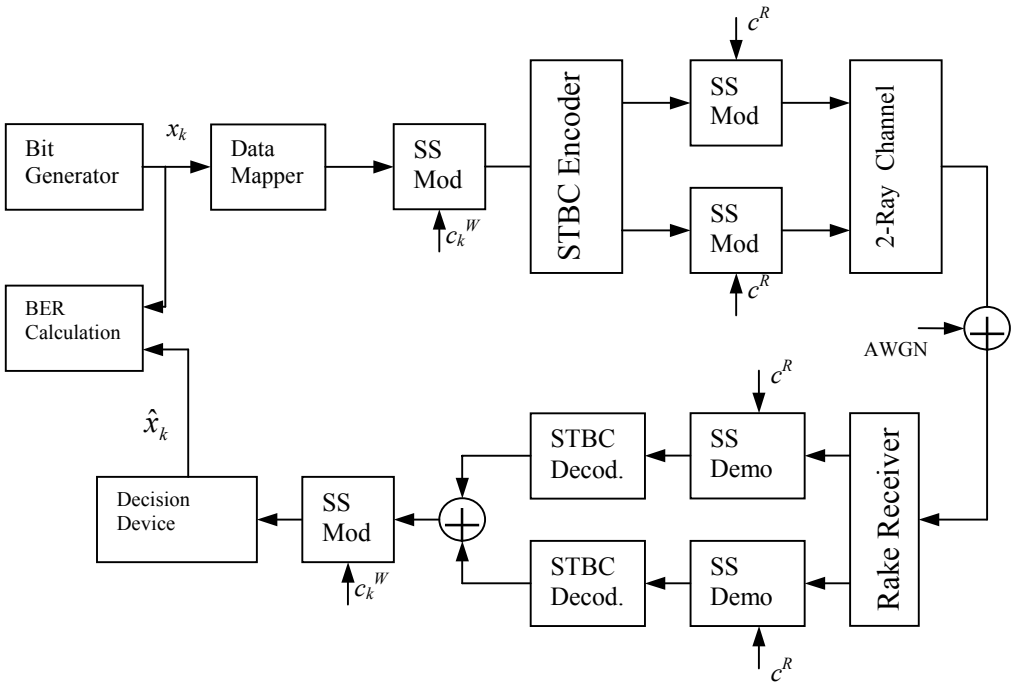

Figure 6.10 Space-time coding-assisted double spread system.

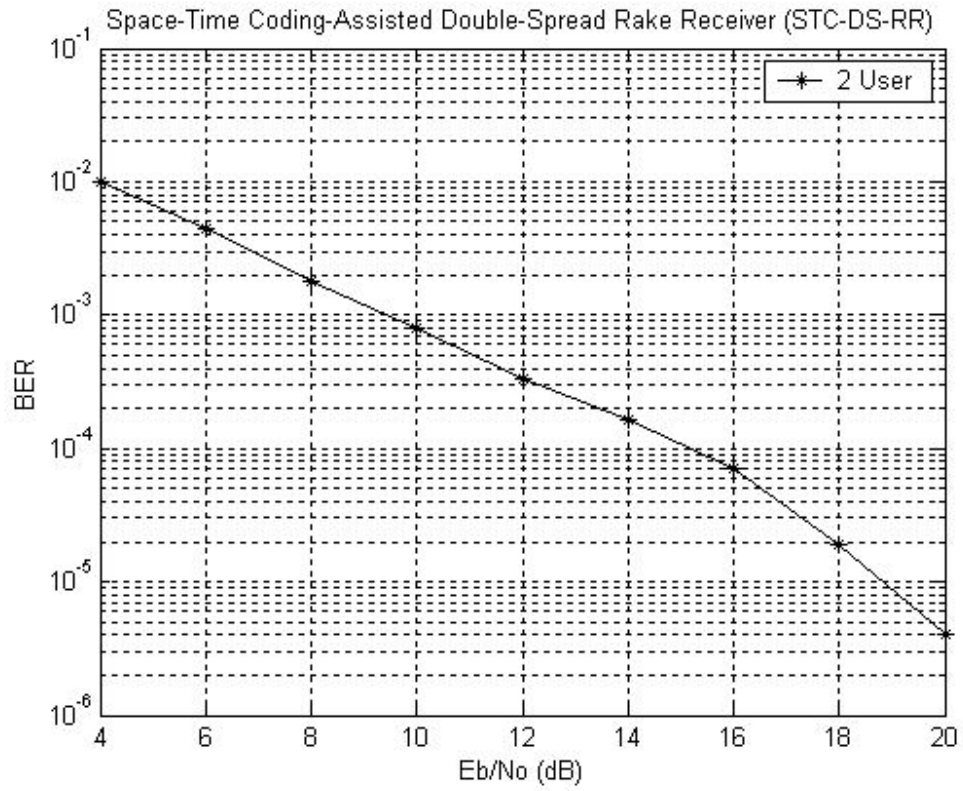

Figure 6.11 Performance of STC-DS-RR case for 2 users

6.8 Performance Comparison of STTD to OTD and STS

It is clearly seen from the Figure 6.12 that STTD and STS outperform OTD. Performances of the STTD and STS are exactly the same but the only difference between these two is the complexity of the transmitter and receiver. Although STS and STTD have different transmit encoder schemes, at output of the two antennas both of the system have same encoded symbols. The reason of bad performance of the OTD system with respect to the STS and STTD is that OTD system has not a full rank spreading code matrix, which means that one of the transmitter antenna while sending information another waiting on idle mode.

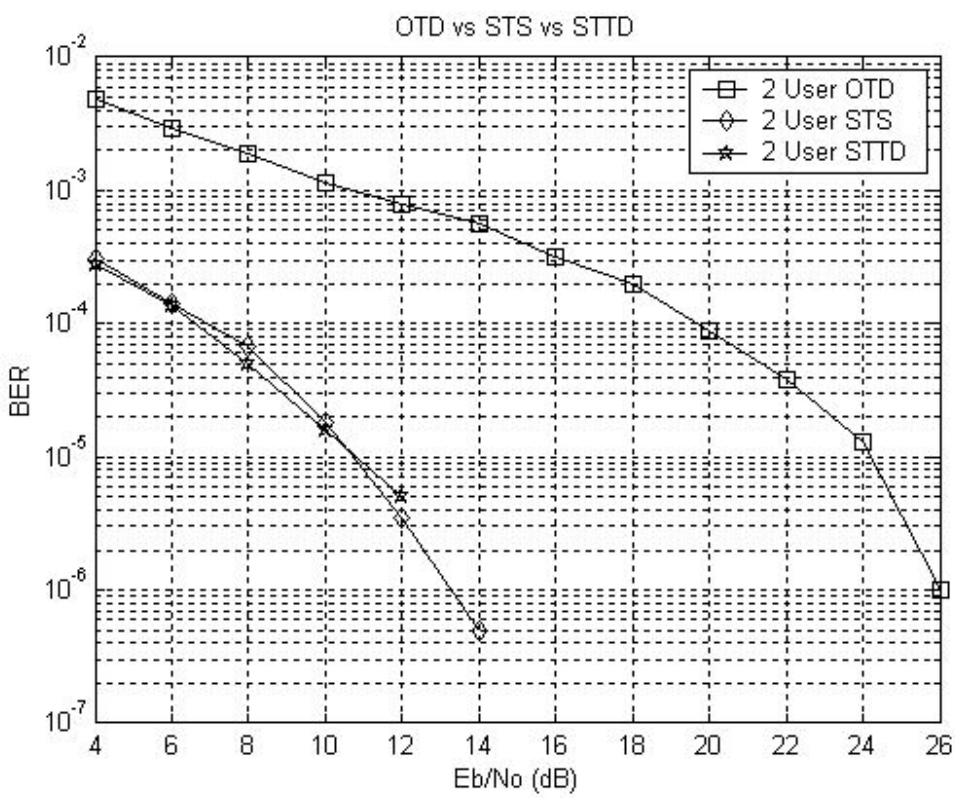

Figure 6.12 Performance comparison of the STTD STS and OTD systems

6.9 Performance Comparison of NTD to STC-DS-RR

Let us now compare the performance of the STC-DS-RR system to the conventional spreading system. Figure 6.13 shows the BER versus the SNR per information bit (E_b/N_0) of both the double spreading and conventional spreading schemes in a multiuser scenario for transmissions over the same channels. Although STC-DS-RR schemes a superior performance with respect to the NTD system this is the trade-off between the number of users and performance. As we explained in section 5.3.3 and 5.3.3.1, total spreading gain in STC-DS-RR system depends on multiplication of the two spreading code lengths and first spreading code length determines maximum number of users. In conventional spreading scheme, we have only one spreading code and the length of this code determines the maximum number of users. In these circumstances, conventional system supports many users than the STC-DS-RR system while total spreading is equal.

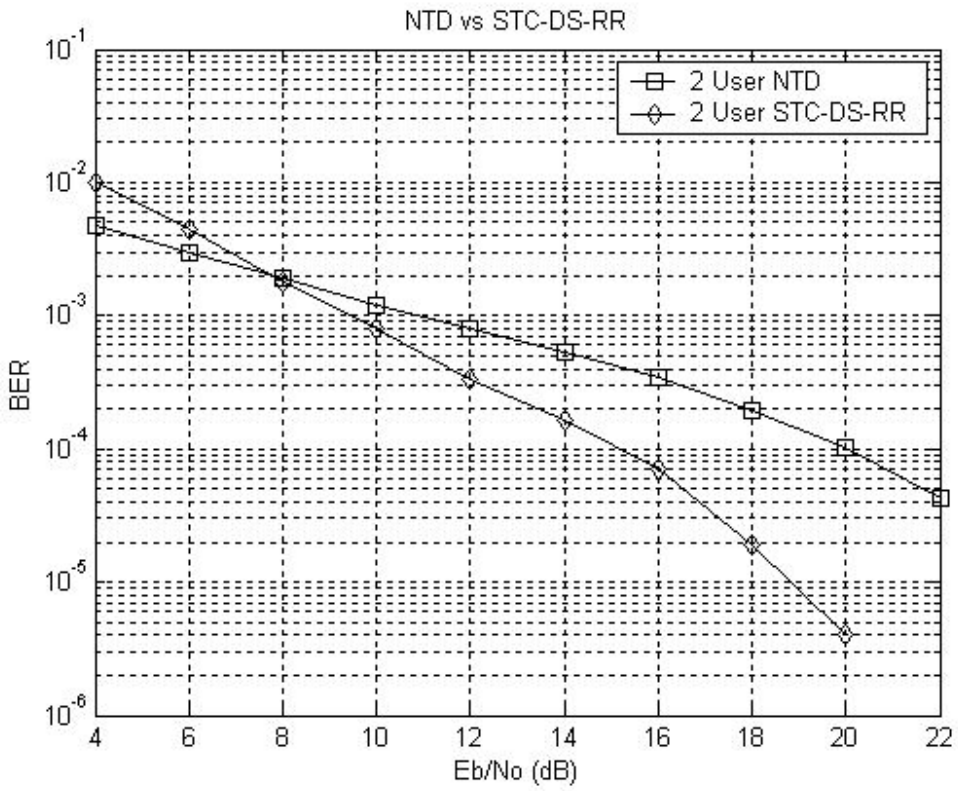

Figure 6.13 Performance comparison of the NTD and STC-DS-RR systems

C H A P T E R 7

CONCLUSIONS

The space-time block coding based transmit diversity scheme was originally proposed for TDMA systems with flat fading channels [3]. Texas Instruments applied it to multipath WCDMA systems and called it the space-time transmit diversity (STTD) [33], [34]. The third generation partnership project (3GPP) accepted STTD as the only open loop transmit diversity scheme in January 1999. After STTD was accepted by the 3GPP, the space-time spreading (STS) was proposed by Lucent for the CDMA 2000 which has accepted both Motorola's orthogonal transmit diversity (OTD) and STS as the open loop transmit diversity techniques.

The interest of this thesis was to investigate and compare existing methods on open loop transmit diversity techniques for next generation wireless networks.

Results from this study indicate that the performance of the STTD and STS is better than OTD in the flat fading channel. Performance of STTD and STS schemes are almost the same. In multipath environment STC-DS-RR open loop transmit diversity scheme gives better performance compared to conventional CDMA system. Another point to consider in comparison is the orthogonality of the Walsh codes. In our simulation, we assume that the codes are orthogonal but in reality this assumption is not true. Due to the increased number of users, the orthogonality of the Walsh codes used by the conventional spreading scheme will be destroyed by the multipath environment. By contrast, the double spreading scheme has no performance degradations when supporting up to 4 users. Hence the orthogonality of the 4 chip Walsh codes was preserved by the double spreading scheme.

In this thesis, a flat fading Rayleigh channel and a two-ray multipath Rayleigh channel model were used for different transmit diversity schemes. For the future work, same simulations can be ran different channel models such as fast fading and more than two-ray multipath channel models. Of course, in such severe channel models performances of the systems will decrease. In order to gain these performance losses, we must look for some other techniques. One is space-time differentially coded CDMA systems [35] [36], another is closed loop techniques, that can be used for such channels.

REFERENCES

[1] Jhong Sam Lee, Leonard E. Miller, CDMA Systems Engineering Handbook, Artech House, 1998.

[2] E. Dahmann, B. Gudmundson, M. Nilsson, and J. Sköld. UMTS/IMT-2000 Based on Wideband CDMA. *IEEE Commun. Mag.,* pages 70-80, Septenber 1998.

[3] S. M. Alamuti. "A Simple Transmit Diversity Technique For Wireless Communications." *IEEE Journal on select. Areas in Commun.,* pages 1451-1458, October 1998.

[4] J. H. winters. "The Diversity Gain of Transmit Diversity in Wireless Systems With Rayleigh Fading." *IEEE Trans. On vehic. Technol*., pages 119-123, February 1998.

[5] 3rd Generation Partnership Project. "Technical Specification Radio Access Network Phisical Layer Procedures." 3GPP TS 25.214 V3.0.0. October 1999.

[6] D. K. Cheng, *Field and Wave Electromagnetics*, Addison-Wesley, New York, 1983.

[7] T. S. Rappaport, *Wireless Communications: Principles and Practice,* Prentice Hall, 1996.

[8] B. Sklar, "Rayleigh Fading Channels in Mobile Digital Communication Systems Part I: Characterization," *IEEE Commun. Mag.,* pp 136-146, Sep. 1997

[9] Ramjee Prasad, Universal Wireless Personal Communications, Artech House, 1998

[10] Savo Glisic, Branka Vucetic, Spread Spectrum CDMA Systems for Wireless Communications, Artech House, 1997.

[11] Gordon L. Stuber, Principles of mobile communication, Kluwer Academic Publishers, 2nd edition, 2001

[12] Tero Ojanperä, Ramjee Prasad, Wideband CDMA for Third Generation Mobile Communications, Artech House, 1998

[13] Michael B. Pursley, Performance Evaluation for Phase-Coded Spread-Spectrum Multiple-Access Communication, *IEEE Transactions on Communications*, Vol.Com-25, No. 8, August 1977

[14] Robert C. Dixon, Spread Spectrum Systems with Commercial Applications, 3nd edition, 1994, John Wiley & Sons

[15] Price, R., and P.E. Green "A Communication Technique For Multipath Channels," *Proc. IRE*, Vol. 46, 1958, pp. 555-570

[16] Gilhousen, K., I. Jacobs, R. Padovani, A. Viterbi, L.Weaver, and C. Wheatley, "On The Capacity Of A Celllar Cdma System*," IEEE Trans. On Vehicular Technology*, Vol.40, No. 2, May 1991, pp. 303-312.

[17] V. Tarokh, N. Seshadri, and A.R. Calderbank, "Space-time codes for high data rate wireless communication: Performance criterion and code construction," *IEEE Trans. Inform. Theory*, vol. 44, no. 2, pp. 744-765, Mar. 1998.

[18] V. Tarokh, A. Naguib, N. Seshadri, and A.R. Calderbank, "Space-time codes for high data rate wireless communication: Performance criteria in the presence of channel estimation errors, mobility, and multiple paths," *IEEE Trans. Comm.*, vol. 47, no.2, pp. 199-207, Feb. 1999.

[19] V. Tarokh, H. Jafarkhani, and A.R. Calderbank, "Space-time block coding for wireless communications: Performance results," *IEEE JSAC,* vol. 17, no. 3, pp. 451-460,March 1999.

[20] W. C. Jakes, *Microwave Mobile Communications*, New York: IEEE Press,1974.

[21] TIA/EIA IS-2000 Physical Layer Specification for CDMA Spread Spectrum Communications System, June 2000.

[22] S.X.Ng, L-L. Yang. T.H. Liew and L. Hanzo, "Space-Time Coding-Assisted Double-Spread Rake Receiver-Based CDMA For Dispersive Rayleigh Fading Environment," *," IEEE Trans. On Vehicular Technology*, Spring, 2002.

[23] G. J. Foschini, and M. J. Gans, "On Limits of Wireless Communications in a Fading Environment When Using Multiple Antennas," *Wireless Pers. Commun.*, Mar. 1998, pp. 311–35.

[24] E. I. Telatar, “Capacity of Multi-Antenna Gaussian Channels,” AT&T Bell Labs. tech. rep., June 1995.

[25] V. Tarokh, H. Jafarkhani, and A. R. Calderbank, “Space- Time Block Codes from Orthogonal Designs,” *IEEE Trans. Info. Theory*, vol. 45, July 1999, pp. 1456–67.

[26] S. Bäro, G. Bauch, and A. Hansmann, “Improved Codes for Space-time Trellis-coded Modulation,” *IEEE Commun. Lett.*, vol. 4, Jan. 2000, pp. 20–2.

[27] C.Papadias, B. Hochwald, T. Mazetta, M. Buehrer and R. Soni, “Space-time spreading for CDMA systems,” *6th Workshop On Smart Antennas In Wireless Mobile Communications*, Standford, CA, July 22-23, 1999.

[28] B. Hochwald, T. Mazetta, and C.Papadias, “A novel space-time spreading scheme for wireless CDMA systems,” *37th Annual Allerton Conference On Communication, Control, And Computing*, Urbana, IL, Sept. 22-24, 1999.

[29] M. Harrison and K. Kuchi, “Open and Closed Loop Transmit Diversity at High Data Rates on 2 and 4 Elements,” 3GPP2-C30-19990817-017, Portland, OR, 1999.

[30] B. Raghothaman *et al.*, “Performance of Simple Space Time Block Codes for More than Two Antennas,” *Proc. Allerton Conf. Commun., Control and Comp.*, Oct. 2000.

[31] D. Gerlach and A. Paulraj, “Adaptive Transmitting Antenna Arrays with Feedback,” *IEEE Sig. Proc. Lett.*, vol. 1, no. 10, Oct. 1994, pp. 150–52.

[32] S. Gurunathan K. Feher, “multipath simulation models for mobile radio channels,” *IEEE* 1992

[33] Texas Instruments, “Space Time Block Coded Transmit Antenna Diversity for WCDMA,” Tdoc 662/98, ETSI SMG 2,L1, Espoo, Finland, December 1998.

[34] Texas Instruments, “Additional Results on Space Time Block Coded Transmit Antenna Diversity for WCDMA,” Tdoc 25/99, ETSI SMG 2,L1, Espoo, Finland, January 1999.

[35] Kun Wang, Hongya Ge, “A new space-time differentially coded DS-CDMA transceiver system for reliable communications,” Acoustics, Speech, and Signal Processing, IEEE International Conference on, vol.3, pp.2793-2796 2002

[36] Jianhua Liu, Jian Liu, “Differential space-time modulation schemes for DS-CDMA systems**,”** Acoustics, Speech, and Signal Processing, Proceedings. 2001 IEEE International Conference on, vol.4 pp.2457-2460.